CHARACTERIZATION OF "HEAVY" CRUDE COMPONENTS

M. M. Boduszynski

Chevron Research Company, P.O. Box 1627,
Richmond, California 94802-0627

The current trend toward processing petroleum residua or
whole "heavy" crudes requires adequate compositional information to
understand the chemistry of reactions that are involved. Monitor-
ing compositional changes by a mere comparison of operationally
defined fractions or by a determination of "average structures" for
feedstock and product components provides inadequate and frequently
misleading information. (1) Much more detailed compositional data
are needed to unravel the structural transformations which occur
during processing or to explain product properties.

This paper discusses recent results of characterization
work on "heavy" crudes and petroleum residua. The emphasis of this
paper is on distribution of homologous series of compounds, their
molar mass and structure, all as a function of boiling point. The
detailed discussion of the experimental procedures used in this
study is beyond the scope of this paper. It is important to note,
however, that the unique combination of short-path distillation,
high performance liquid chromatography (HPLC), and field ionization
mass spectrometry (FIMS) was essential for obtaining the detailed
compositional information which was not available before. The
nitrogen-rich, 13.6°API gravity, Kern River crude oil (a blend of
crudes from San Joaquin Valley, California) is used as an example.

EXPERIMENTAL

Kern River crude oil was first distilled using a Penn
State column to produce two distillates, Cut 1 and Cut 2, and atmo-
spheric residuum (~650°F+). The residuum was then fractionated
into eight distillates, Cut 3 through Cut 10, and the nondistil-
lable residuum (~1300°F+) using the short-path distillation. The
detailed description of the short-path distillation apparatus,
DISTACT, can be found elsewhere. (2, 3) The true boiling point
(TBP) distributions of the distillation cuts were determined using
a vacuum thermal gravimetric analysis (VTGA) method developed at
Chevron Research. (4) The molar mass distributions of all cuts
were determined using FIMS and field desorption mass spectrometry
(FDMS). (5) The FIMS data were obtained at SRI International,

Encl. - Table I
        Figures 1-8

Menlo Park, California. Average molecular weights were determined
by vapor pressure osmometry (VPO) using toluene as a solvent.
Carbon (C), hydrogen (H), sulfur (S), total nitrogen (N_t), basic
nitrogen (N_b), and oxygen (O) were determined using standard proce-
dures. Nickel (Ni), vanadium (V), and iron (Fe) were determined by
inductively coupled plasma (ICP) emission spectroscopy method.

Chromatographic separations of all distillation cuts
involved a two-step procedure. First, a fraction of polar compo-
nents (mainly N-, O-, and metal-containing compounds) was isolated
from each distillation cut before further HPLC separation to pre-
vent possible damage of high efficiency columns. "Polars" were
separated using liquid chromatography on basic alumina. In the
second step, the "polars-free" fraction was further separated into
saturates, monoaromatics, diaromatics, triaromatics, tetraaro-
matics, pentaaromatics, and a fraction designated "hexaaromatics
and/or azarenes."

The HPLC system consisted of two preparative columns,
ZORBAX-NH$_2$ and ZORBAX-SIL, connected through a switching valve.
The system was calibrated using model compounds. The actual cut
points between the aromatic ring-type fractions were determined
using ultraviolet (UV) spectra collected from 200-400 nm by the UV
photodiode array detector at 20-sec. intervals. Weight percent
yields of the fractions were determined gravimetrically. The HPLC
fractions were analyzed by FIMS. The principles of the HPLC/FIMS
approach and its application to characterization of coal-derived
liquids were reported previously. (6-8) However, a different HPLC
system was used in this study. Elemental analysis, infrared spec-
trometry, ^{1}H and ^{13}C nuclear magnetic resonance (NMR) spectrometry,
and EIMS were used occasionally to aid interpretation of the
HPLC/FIMS data.

RESULTS AND DISCUSSION

How Heavy is the
"Heavy" Crude Oil?

The adjectives "heavy," "high boiling," and "high molecu-
lar weight" are commonly but inappropriately used as equivalent
terms to describe crude oils or their fractions. The term "heavy"
refers to crude oil density. Heavy crudes, of which Boscan
(10.1°API gravity in Figure 1) is a classic example, have high
densities (low °API gravities) because they are rich in high
density naphthene-aromatics and heteroatom-containing compounds and
poor in low density alkanes. They are commonly either immature or
degraded. (9) Light crudes, which have low densities (high °API

gravities) are rich in alkanes. Altamont crude oil (42.2°API gravity in Figure 1), an extreme example, has an exceptionally high alkane content as a result of its predominant source being lacustrine algae, which also happens to have been the source of the nearby Green River shale. (9)

For each of the crudes considered in Figure 1, the °API gravity decreases with increasing depth of distillation. Hence the term "heavy ends" tends to correlate with "high boiling" within a given crude. However, the correlation between "heavy" and "high boiling" does not necessarily hold if different crudes are being compared. For example, the nondistillable residuum (~1300°F+) from Altamont crude has a lower density (higher °API gravity) than whole Boscan, Kern River, or Maya crude.

The terms "heavy" and "high boiling" are frequently but incorrectly used as if they were synonymous with "high molecular weight." The boiling point of a compound at a given pressure is a rough measure of the attractive forces between the molecules. These forces vary with the structure of molecules, leading to the great differences in boiling point for compounds of a given molar mass but a different chemical structure. This is illustrated in Figure 2. Compounds having similar molar masses cover a broad boiling point range and, conversely, a narrow boiling point cut contains a wide molar mass range. The molar mass range increases rapidly with increasing boiling point, as illustrated by the extended curves "A" and "C" at the right side of Figure 2. For a given class of compounds, the boiling point increases with molar mass. This is due to the increase of the weak, van der Waals attractive intermolecular forces as molecules of a given type become larger. However, compounds having fused aromatic rings and functional groups capable of hydrogen bonding or other types of polar interactions have additional attractive intermolecular forces and may have a relatively low molar mass but a high boiling point and thus are expected to concentrate in the "heavy ends."

Figure 3 shows boiling point, molar mass, and heteroatom distributions in Kern River petroleum. The apparent molar mass distributions of all distillation cuts, including the nondistillable residuum, were measured by FIMS and FDMS. The results obtained by both techniques were in very good agreement. The molar mass distributions are illustrated in Figure 3 by using the molar mass scale as a radius of each "slice." The radius of the inner circle corresponds to the lowest molar mass of that cut while the radius of the outer circle extends to the highest molar mass value. A significant trend can be observed. The molar mass range of the successive distillation cuts widens with increasing boiling

point in a fashion that is consistent with the trend indicated by the curves in Figure 2. The low molar mass end of each cut (radius of the "hole" in each slice) shows only a moderate increase with increasing boiling point while the high molar mass end soars. The resulting significant molar mass overlapping between the cuts is mainly due to the increasing concentration of polynuclear aromatic and heteroatom-containing compounds which have high boiling points but relatively low molar masses.

Interestingly, most of these heavy crude components do not exceed a molar mass of about 1500 and only a few have molar masses extending up to about 1900. The molar mass data for Kern River crude oil are in agreement with the previously reported results for other crudes (10-12) and provide further support for the early speculations by Dean and Whitehead (13) who suggested a molecular weight maximum of 2000 for all compounds in petroleum.

Data in Table I give distributions of elements (C, H, N, S, O, Ni, and V) on a molecular basis. The decreasing Z value in the general formula $C_nH_{2n+z}X$ for each successive cut indirectly indicates the increasing "aromaticity." The C number range and the concentration of heteroatom-containing molecules also increase with increasing boiling point. For example, the low boiling Cut 1 (385-499°F) consists of molecules having about 10-14 C atoms, with only two molecules in 100 containing S and one in 1000 containing a N atom. The high boiling Cut 5 (795-943°F) involves molecules having about 18-48 C atoms and on the average every other molecule may contain a heteroatom. The nondistillable residuum has the highest concentration of heteroatoms and shows the greatest H deficiency (lowest Z value) among all distillation cuts. One must bear in mind, however, that the above are only average estimates which cannot reveal the actual distribution of heteroatoms in the diverse molecules present in each cut.

What are the Components of a "Heavy" Crude Oil?

The complexity of petroleum increases rapidly with increasing boiling point as the result of the increasing number of atoms in a molecule and the immense number of their possible structural arrangements. It has long been recognized that compositional analysis of high boiling petroleum fractions by the isolation of individual compounds is a practical impossibility. (14) Instead, many attempts have been made to separate those complex mixtures into groups or classes of compounds. Numerous separation methods and schemes have been developed over the years. (15) One of the most recent systematic studies on composition of petroleum high

boiling distillates and residua was the American Petroleum
Institute Research Project 60 and the later work based on the char-
acterization scheme developed under this project. (10-12, 16-22)

Petroleum components can be viewed as two major groups of
compounds, namely, hydrocarbons and nonhydrocarbons. Hydrocarbons
include acyclic alkanes (paraffins) and cycloalkanes (naphthenes),
both commonly referred to as saturates, and the third group known
as aromatics. Most of the aromatics bear normal or branched chains
and naphthenic cycles. A molecule containing one aromatic ring is
regarded as monoaromatic, a molecule with two aromatic rings--
diaromatic, etc., even if several naphthenic rings and side chains
are attached to the aromatic ring. In the same manner, naphthenes
containing both saturated rings and chains are defined by the
number of rings, i.e., monocyclic, dicyclic, etc. Nonhydrocarbons
include compounds which in addition to C and H atoms also involve
one or several heteroatoms such as S, N, O, Ni, V, and Fe.

A complete separation of hydrocarbons from nonhydrocar-
bons in high boiling petroleum fractions is not possible.
S-containing compounds which during chromatographic separations
behave similarly to hydrocarbons of the equivalent molar structure
(i.e., dibenzothiophene and fluorene) are commonly found in hydro-
carbon fractions. Some N heterocycles (azarenes), particularly
those with the N atom sterically hindered or N-substituted, also
frequently interfere with hydrocarbons. Nonhydrocarbons having
"polar" functional groups such as -COOH, -OH, -NH, C=O or those
containing several heteroatoms in a molecule (i.e., metalloporphy-
rins) are less difficult to separate from hydrocarbons.

The separation method used in this study produced up to
eight "compound-class" fractions from each distillation cut depend-
ing on the cut composition. The fraction of "polars" which is
regarded as a concentrate of mainly N-, O-, and metal-containing
species was separated from each cut prior to further separations of
the remaining "polars-free" portion into saturates, monoaromatics,
diaromatics, triaromatics, tetraaromatics, pentaaromatics, and a
fraction designated "hexaaromatics and/or azarenes." The last
fraction reflects the difficulty in separating polycyclic aromatic
hydrocarbons having six or more rings from azarenes.

It is important to note, however, that even the most
sophisticated HPLC system cannot provide a complete separation and
the adjacent fractions therefore show some overlapping. This, how-
ever, is detected by the following FIMS analysis of the fractions.
The FIMS provides further "separation" into various homologous
series according to the Z value in the general formula C_nH_{2n+Z} and
reveals the molar mass (C number) distribution of the components.

The structural assignments are based on the HPLC retention data, UV spectra (for aromatics), and if necessary are aided by such analytical techniques as ^1H and ^{13}C NMR, and EIMS.

Figures 4, 5, and 6 show examples of the HPLC/FIMS analyses for distillate Cuts 2, 6, and 10, respectively. Only a few most prominent homologous series are presented. Most likely structures are shown although various isomers are possible. The extensive compositional information provided by this analytical approach is evident. Of particular importance are series of polycyclic molecules many of which are related to steroid and terpenoid structures ranging from the saturated form to various stages of aromatization.

The earlier discussed effect of chemical structure on molar mass distribution for components of a given distillation cut is illustrated in Figure 5. The molar mass profile of acyclic alkanes shows the maximum at C_{39} while that of the pentaaromatic C_nH_{2n-30} series has the maximum at C_{30}. Molar mass profiles of "polars" (not shown) were "shifted" even further toward lower molar mass values than those of the corresponding hydrocarbons but showed similar patterns in terms of wide C number distributions. The interpretation of the FIMS data for "polars" is much more difficult than in the case of hydrocarbons, particularly if more than one heteroatom per molecule is involved. Infrared and NMR data, together with elemental analysis results, provided important additional information. Compounds having pyrrolic NH groups (i.e., carbazoles) and amide types were found to be particularly abundant. Although various homologous series were identified, the results indicate the need for further separation of "polars" to facilitate the interpretation of data.

Figure 7 shows distributions of various "compound-class" fractions in the heavy Kern River crude oil. The concentration of "polars" increases steadily with increasing boiling point from zero in Cut 1 to about 82 wt % in the nondistillable residuum. Notably, "polars" in the distillable portion (Cut 1 through Cut 10) account for over 42% of total "polars" present in this heavy crude oil. The mono- through pentaaromatics and the fraction designated "hexa-aromatics and/or azarenes," together show a peculiar distribution pattern with two minima, one at the top and the other at the bottom of the barrel. The concentrations of individual fractions vary in each successive distillation cut. The mono- and diaromatics predominate in the low boiling cuts. It is worthwhile noting, however, that the composition of the individual fractions within these classes changes considerably with increasing boiling point. For example, the monoaromatics in Cut 2 are rich in di- and

tricyclomonoaromatics (homologous series C_nH_{2n-8} and C_nH_{2n-10}) while the monoaromatics in Cut 4 involve mainly tri-, tetra-, and pentacyclomonoaromatics (homologous series C_nH_{2n-10}, C_nH_{2n-12}, and C_nH_{2n-14}).

The data in Figure 7 show a dramatic decrease in saturates with increasing boiling point from about 88 wt % in Cut 1 to only about 1 wt % in the nondistillable residuum. Similarly, as with other compound-class fractions, the composition of saturates changes with increasing boiling point. This is illustrated in Figure 8 which shows distributions of the alkane homologous series in the entire Kern River crude oil. Acyclic alkanes (paraffins) are almost completely absent in this degraded heavy crude oil. The concentrations of tetra-, penta-, and hexacyclics increase with increasing boiling point at the expense of mono-, di-, and tri-cyclic alkanes. Steranes and hopanes were found to be particularly abundant in Cuts 3 through 6.

CONCLUSIONS

Data derived from this study dispel many misconceptions about the composition of high boiling components in petroleum. The results presented show that the molecular structure more than molecular weight of petroleum components predominantly determines the boiling point distribution and density (°API gravity) of the crude oil. The majority of compounds found in the "heavy" Kern River crude oil have molar masses not exceeding about 1500 with only a few extending up to about 1900. They involve mainly polycyclic structures with varying degree of aromatization, and many of them contain N and O atoms with pyrrolic and amide types prevailing.

The results of this study also demonstrate the necessity of a high degree of sample fractionation in order to obtain meaningful compositional information.

REFERENCES

1. Boduszynski, M. M., "Liquid Fuels Technology," 2 (3), 211-232 (1984).

2. Vercier, P., and Mouton, M., "Analusis," 101 (2), 57-70 (1982).

3. Fischer, W., "Decomposition-Free Distillation of Crude Oil Fractions with Boiling Ranges of 350-700°C," Leybold-Heraeus GmbH, Hanau, Germany.

4. Su, F., unpublished results.

5. Rechsteiner, C. E., unpublished results.

6. Boduszynski, M. M.; Hurtubise, R. J.; Allen, T. W.; and Silver, H. F., "Anal. Chem.," 55, 225-231 (1983).

7. Boduszynski, M. M.; Hurtubise, R. J.; Allen, T. W.; and Silver, H. F., "Anal. Chem.," 55, 232-241 (1983).

8. Boduszynski, M. M.; Hurtubise, R. J.; Allen, T. W.; and Silver, H. F., Fuel, in Press.

9. Tissot, B. P., and Welte, D. H., "Petroleum Formation and Occurrence," Springer-Verlag, Berlin, Heidelberg, New York (1978).

10. McKay, J. F., and Latham, D. R., Preprints, ACS, Div. Petrol. Chem., 26 (4), 831-838 (1981).

11. Boduszynski, M. M.; McKay, J. F.; and Latham, D. R., Preprints, ACS, Div. Petrol. Chem., 26 (4), 865-881 (1981).

12. Boduszynski, M. M.; McKay, J. F.; and Latham, D. R., Proc. Assn. Asph. Pav. Technol., 49, 123-142 (1980).

13. Dean, R. A, and Whitehead, E. V., Proc. Sixth World Petroleum Congress, Sec. V, Paper 9, 261-276 (1963).

14. Van Nes, K., and Van Westen, H. A., "Aspects of the Constitution of Mineral Oils," Elsevier Publishing Co., Inc., New York, Amsterdam, London, Brussels (1951).

15. Altgelt, K. H.; Jewell, D. M.; Latham, D. R.; and Selucky, M. L., "Chromatography in Petroleum Analysis," Chapter 9, 195-214, Altgelt, K. H., and Gouw, T. H., editors, Marcel Dekker, Inc., New York, Basel (1979).

16. Haines, W. E., and Thompson, C. J., "Separating and Characterizing High Boiling Petroleum Distillates: the USBM-API Procedure," Rept. of Inv. LERC/RI-75/5, BERC/RI-75/2, (1975).

17. Thompson, C. J.; Ward, C. C.; and Ball, J. S., "Characteristics of World's Crude Oils and Results of API Research Project 60," Rept. of Inv. BERC/RI-76/8 (1976).

18. McKay, J. F.; Amend, P. J.; Harnsberger, P. M.; Cogswell, T. E.; and Latham, D. R., Fuel, 60, 14-16 (1981).

19. McKay, J. F.; Harnsberger, P. M.; Erickson, R. B.; Cogswell, T. E.; and Latham, D. R., Fuel, 60, 17-26 (1981).

20. McKay, J. F.; Latham, D. R.; and Haines, W. E., Fuel, 60, 27-32 (1981).

21. Grizzle, P. L.; Green, J. B.; Sanchez, V.; Murgia, E.; and Lubkowitz, L., Preprints, ACS, Div. Petrol. Chem., 26 (4) 839-850 (1981).

22. Sturm, Jr., G. P.; Grindstaff, Q. G.; Hirsch, D. E.; Scheppele, S. E.; and Hazos, M., Preprints, ACS, Div. Petrol Chem., 26 (4) 851-856 (1981).

TABLE I

DISTRIBUTIONS OF C, H, N, S, O, Ni, AND V ATOMS
IN KERN RIVER PETROLEUM

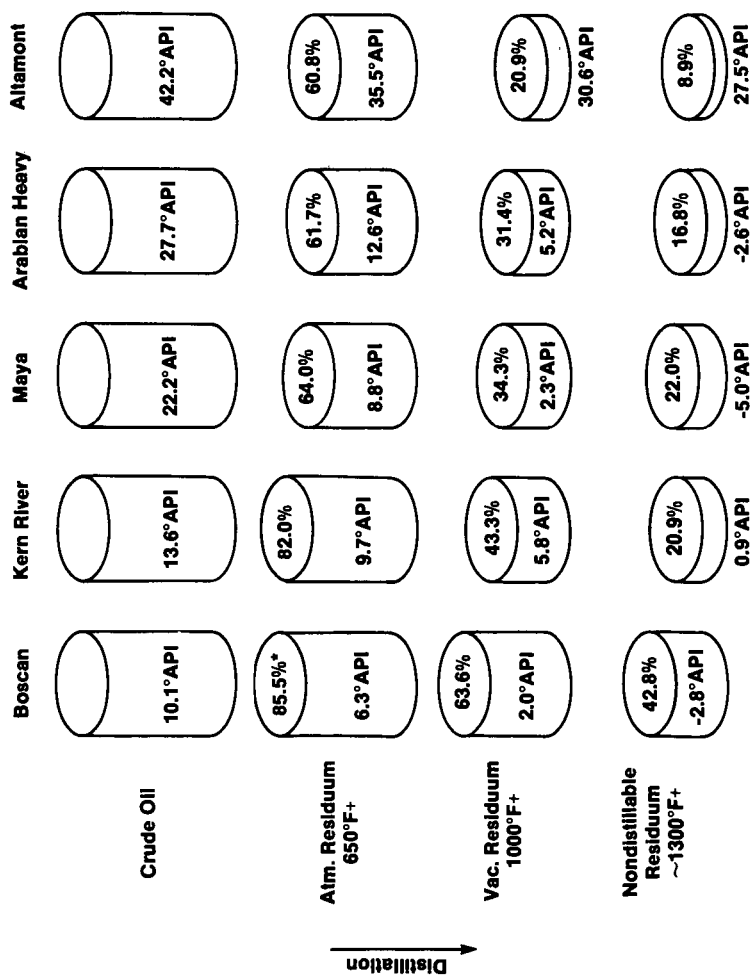| Cut No.[1]	Cumulative Wt % from Crude Oil	Approximate C Atom Range[2]	Average Number of Atoms in Molecule[3]							Total Hetero-atoms	z in C_nH_{2n+z} [4]
			C	H	N	S	O	Ni	V		
1	6.4	10-14	13.2	24.1	0.001	0.02	-	-	-	0.02	-2.3
2	18.0	12-24	17.8	29.9	0.015	0.06	0.05	-	-	0.12	-5.7
3	35.8	14-36	22.6	36.9	0.07	0.10	0.08	-	-	0.25	-8.3
4	45.0	16-42	27.3	43.5	0.12	0.12	0.11	-	-	0.35	-11.1
5	53.2	18-48	30.6	47.8	0.20	0.15	0.16	-	-	0.51	-13.4
6	60.3	20-53	35.7	55.3	0.28	0.18	0.19	2×10^{-5}	3×10^{-6}	0.65	-16.1
7	66.0	22-62	41.7	63.8	0.35	0.24	0.26	3×10^{-4}	8×10^{-5}	0.85	-19.6
8	70.9	25-71	47.0	71.1	0.47	0.29	0.39	1.3×10^{-3}	5×10^{-4}	1.15	-22.9
9	74.7	27-81	52.1	77.9	0.59	0.31	0.43	2×10^{-3}	9×10^{-4}	1.34	-26.3
10	79.1	29-93	58.5	87.4	0.70	0.33	0.48	1.4×10^{-3}	7×10^{-4}	1.51	-29.6
Nondistillable Residuum	100.0	32-134	84.8	116.4	1.49	0.54	0.82	5×10^{-3}	3×10^{-3}	2.86	-53.2

[1] See Figure 3.

[2] From FIMS and wt % C data.

[3] Calculated using average molecular weight value by FIMS and elemental analysis results.

[4] x = heteratom(s).

3-8-85

FIGURE 1

THE EFFECT OF DISTILLATION ON API GRAVITY FOR VARIOUS CRUDE OILS

	Boscan	Kern River	Maya	Arabian Heavy	Altamont
Crude Oil	10.1°API	13.6°API	22.2°API	27.7°API	42.2°API
Atm. Residuum 650°F+	85.5%* 6.3°API	82.0% 9.7°API	64.0% 8.8°API	61.7% 12.6°API	60.8% 35.5°API
Vac. Residuum 1000°F+	63.6% 2.0°API	43.3% 5.8°API	34.3% 2.3°API	31.4% 5.2°API	20.9% 30.6°API
Nondistillable Residuum ~1300°F+	42.8% -2.8°API	20.9% 0.9°API	22.0% -5.0°API	16.8% -2.6°API	8.9% 27.5°API

Distillation →

*Wt % Yield from Crude Oil

375

FIGURE 2
THE EFFECT OF MOLECULAR STRUCTURE ON BOILING POINT

FIGURE 3
BOILING POINT, MOLAR MASS, AND
HETEROATOM DISTRIBUTIONS IN KERN RIVER PETROLEUM (13.6°API)

10-90% TBP, °F	Yield from Crude, Wt %	Cut No.	Average Molecular Weight		Atomic Ratio H/C	Nonmetals, Wt %				Ratio N_b/N_t	Metals, ppm		
			FIMS	VPO		S	O	N_t	N_b		Ni	V	Fe
385-499	8.2	1	184	190	1.628	0.33	-	0.008	-	-	-	-	-
523-642	11.8	2	246	260	1.686	0.79	0.31	0.088	0.058	0.66	-	-	-
637-778	17.8	3	318	337	1.631	0.99	0.42	0.31	0.11	0.35	-	-	-
739-876	9.2	4	381	420	1.598	1.02	0.45	0.46	0.15	0.33	-	-	-
795-943	8.2	5	428	471	1.563	1.11	0.60	0.85	0.17	0.26	-	-	-
858-1011	7.1	6	498	527	1.553	1.19	0.60	0.78	0.21	0.27	2	0.3	0
920-1081	5.7	7	584	594	1.532	1.34	0.71	0.84	0.23	0.27	29	7	0.9
986-1153	4.9	8	859	662	1.514	1.34	0.94	1.01	0.27	0.27	117	40	1.4
1050-1228	4.4	9	730	755	1.496	1.34	0.94	1.14	0.28	0.25	160	65	7
1150-1369	3.8	10	620	876	1.494	1.39	0.95	1.19	0.30	0.25	102	45	8
Nondistillable Residuum	20.9		1200	1916	1.374	1.43	1.10	1.74	0.41	0.24	249	122	183

Heteroatoms

Molar Mass   0   1000   2000
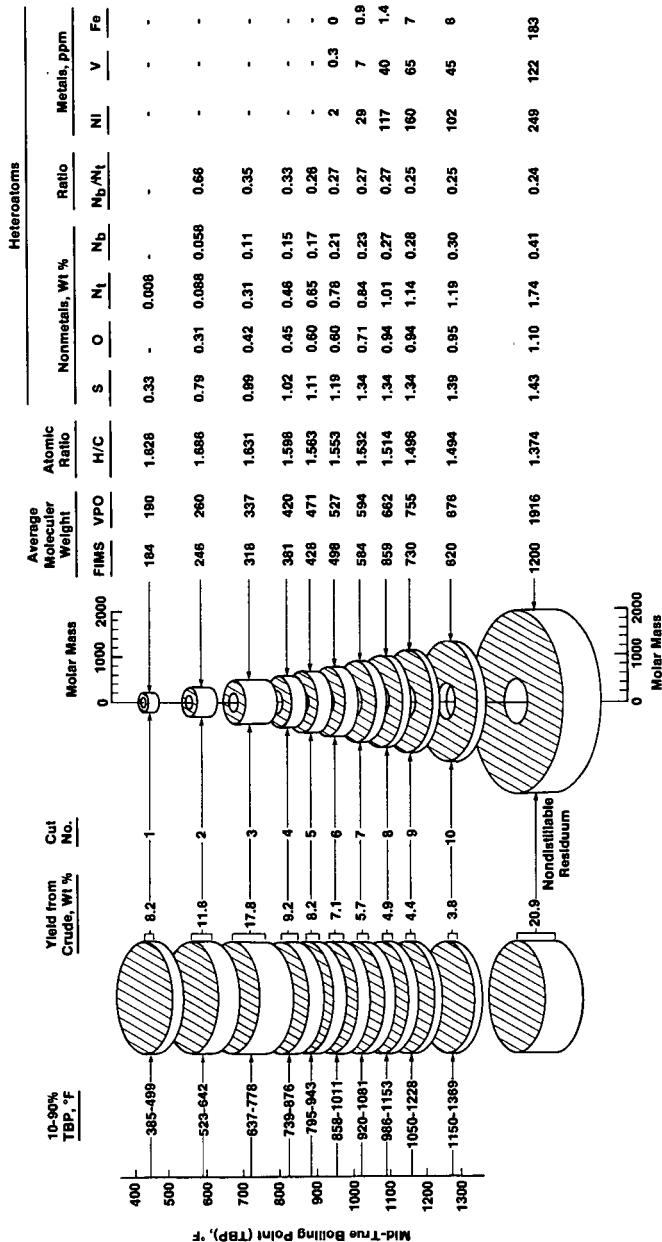
Mid-True Boiling Point (TBP), °F

FIGURE 4

SCHEMATIC DIAGRAM OF HPLC-FIMS ANALYSIS OF CUT 2 (523-642°F) FROM KERN RIVER PETROLEUM

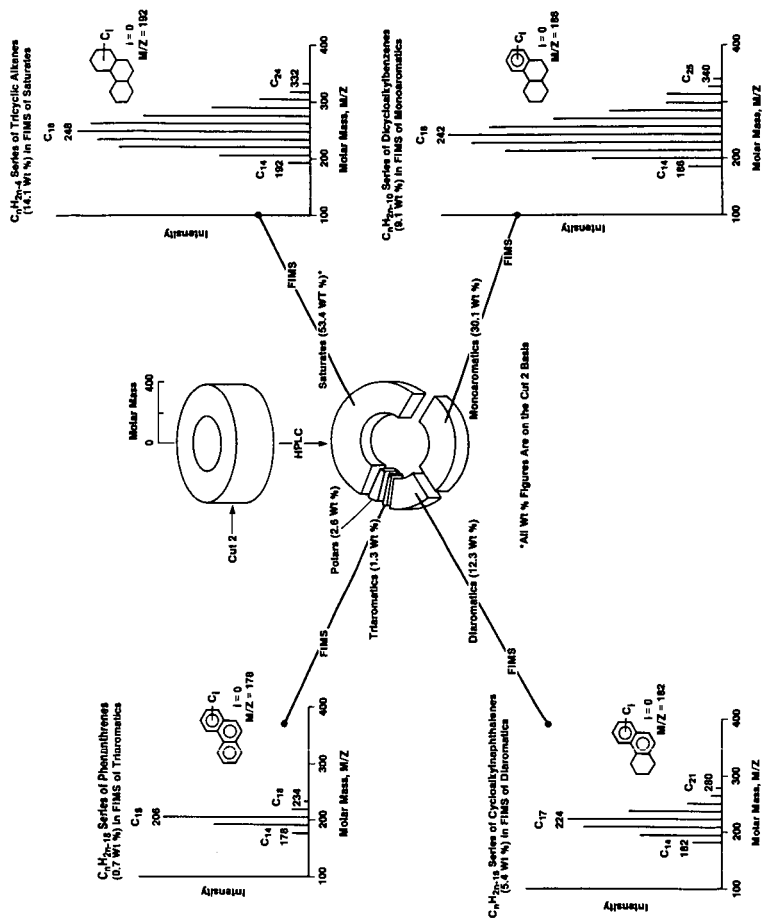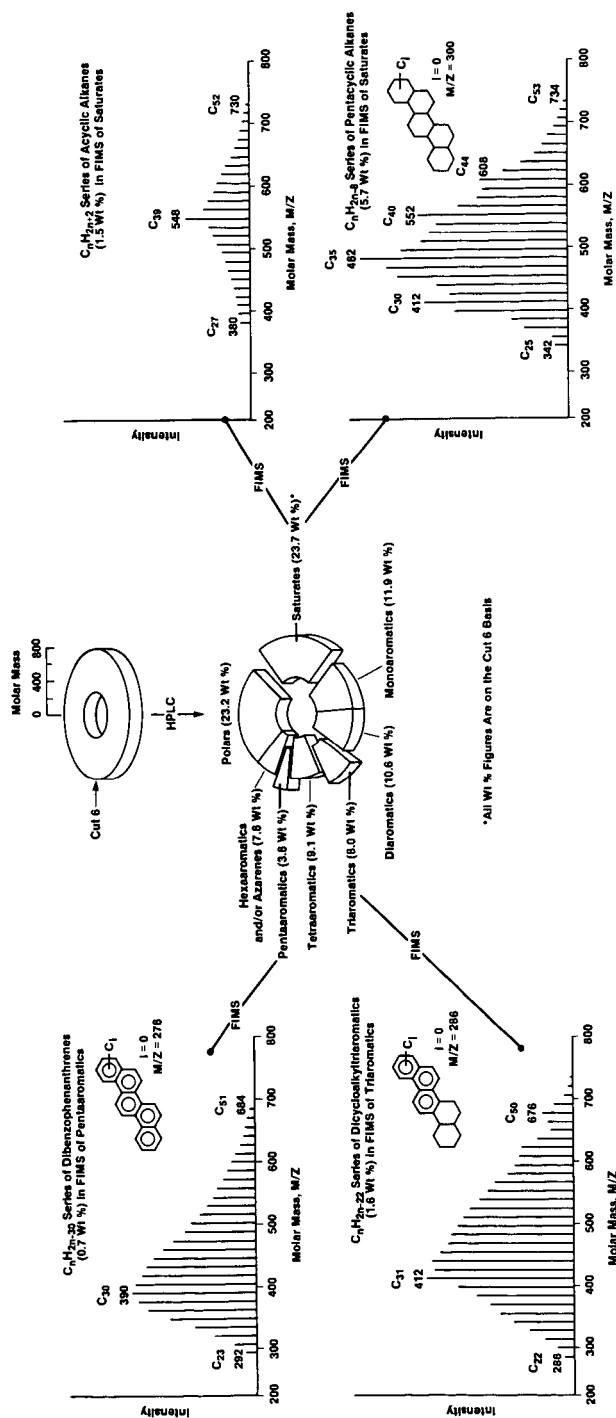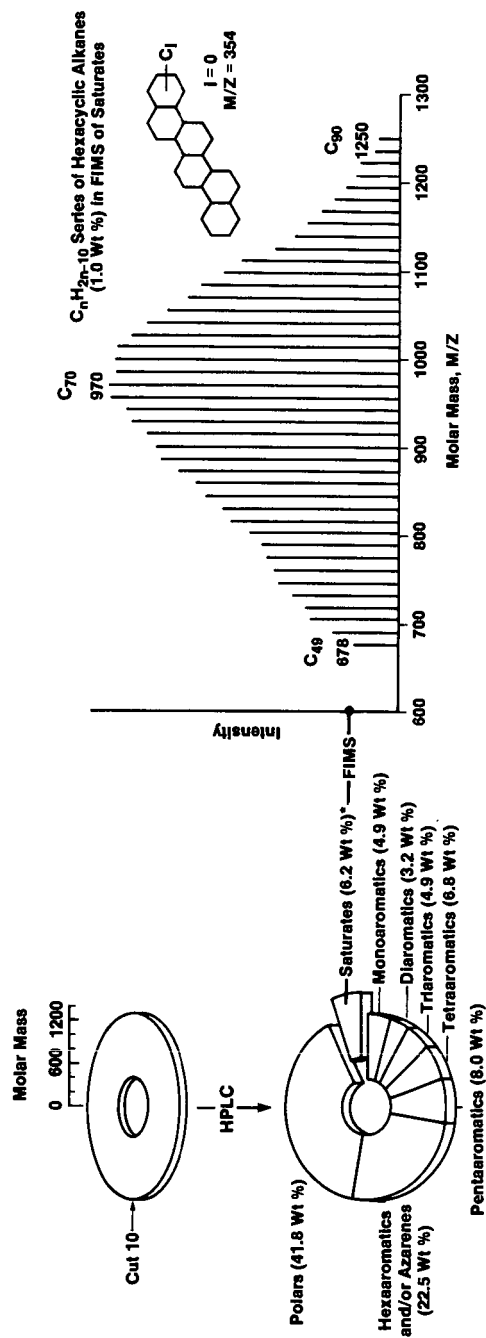### Note: Only Selected Homologous Series Are Shown as Examples

C_nH_{2n-4} Series of Tricyclic Alkanes
(14.1 Wt %) in FIMS of Saturates

I = 0
M/Z = 192

C_{10} 248
C_{14} 192
C_{24} 332

Molar Mass, M/Z

Intensity

100   200   300   400

C_nH_{2n-10} Series of Dicycloalkylbenzenes
(2.1 Wt %) in FIMS of Monoaromatics

I = 0
M/Z = 186

C_{18} 242
C_{14} 186
C_{25} 340

Molar Mass, M/Z

Intensity

100   200   300   400

Molar Mass

0   400

Cut 2

HPLC

Saturates (53.4 Wt %)*

Polars (2.6 Wt %)

Triaromatics (1.3 Wt %)

Diaromatics (12.3 Wt %)

Monoaromatics (30.1 Wt %)

*All Wt % Figures Are on the Cut 2 Basis

FIMS

FIMS

FIMS

FIMS

C_nH_{2n-18} Series of Phenanthrenes
(0.7 Wt %) in FIMS of Triaromatics

I = 0
M/Z = 178

C_{16} 206
C_{14} 178
C_{18} 234

Molar Mass, M/Z

Intensity

100   200   300   400

C_nH_{2n-18} Series of Cycloalkylnaphthalenes
(5.4 Wt %) in FIMS of Diaromatics

I = 0
M/Z = 182

C_{17} 224
C_{16} 182
C_{21} 280

Molar Mass, M/Z

Intensity

100   200   300   400

378

FIGURE 5

SCHEMATIC DIAGRAM OF HPLC-FIMS ANALYSIS OF
CUT 6 (858-1011°F) FROM KERN RIVER PETROLEUM

Note: Only Selected Homologous Series Are Shown as Examples

Molar Mass
0   400   800

Cut 6

HPLC →

Polars (23.2 Wt %)

Hexaaromatics
and/or Azarenes (7.8 Wt %)

Pentaaromatics (3.8 Wt %)

Tetraaromatics (9.1 Wt %)

Triaromatics (8.0 Wt %)

Diaromatics (10.6 Wt %)

Monoaromatics (11.9 Wt %)

Saturates (23.7 Wt %)*

*All Wt % Figures Are on the Cut 6 Basis

C_nH_{2n-30} Series of Dibenzophenanthrenes
(0.7 Wt %) in FIMS of Pentaaromatics

I = 0
M/Z = 278

FIMS

C_{23} 292
C_{30} 390
C_{51} 684
Intensity
Molar Mass, M/Z
200 300 400 500 600 700 800

C_nH_{2n-22} Series of Dicycloalkyltriaromatics
(1.6 Wt %) in FIMS of Triaromatics

I = 0
M/Z = 286

FIMS

C_{22} 288
C_{31} 412
C_{50} 676
Intensity
Molar Mass, M/Z
200 300 400 500 600 700 800

C_nH_{2n+2} Series of Acyclic Alkanes
(1.5 Wt %) in FIMS of Saturates

FIMS

C_{27} 380
C_{30} 548
C_{52} 730
Intensity
Molar Mass, M/Z
200 300 400 500 600 700 800

C_nH_{2n-8} Series of Pentacyclic Alkanes
(5.7 Wt %) in FIMS of Saturates

FIMS

I = 0
M/Z = 300

C_{25} 342
C_{30} 412
C_{35} 482
C_{40} 552
C_{44} 608
C_{53} 734
Intensity
Molar Mass, M/Z
200 300 400 500 600 700 800

FIGURE 6

SCHEMATIC DIAGRAM OF HPLC-FIMS ANALYSIS OF
CUT 10 (1150-1369°F) FROM KERN RIVER PETROLEUM

FIGURE 7

COMPOUND-CLASS DISTRIBUTIONS IN KERN RIVER PETROLEUM
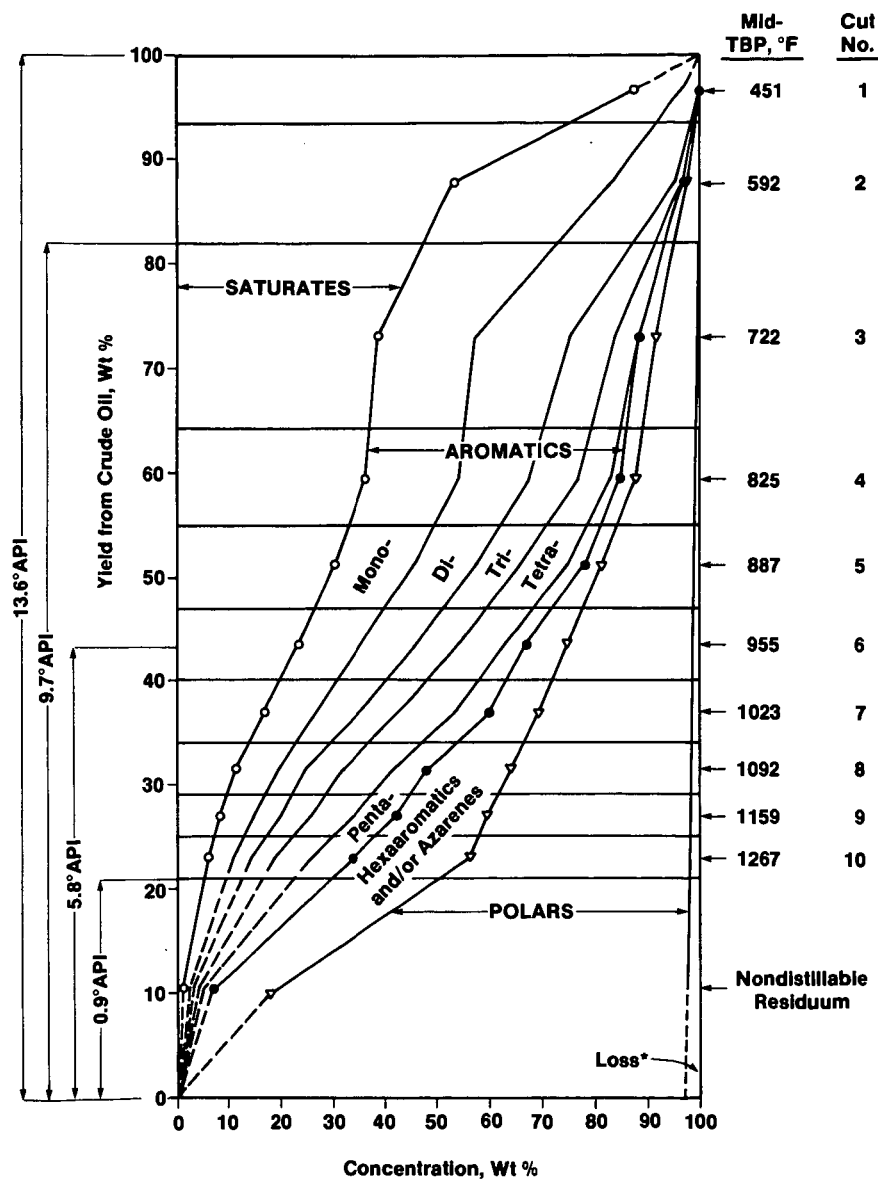
*Unrecovered material during chromatographic separations.

FIGURE 8

DISTRIBUTIONS OF ALKANE HOMOLOGOUS SERIES IN KERN RIVER PETROLEUM
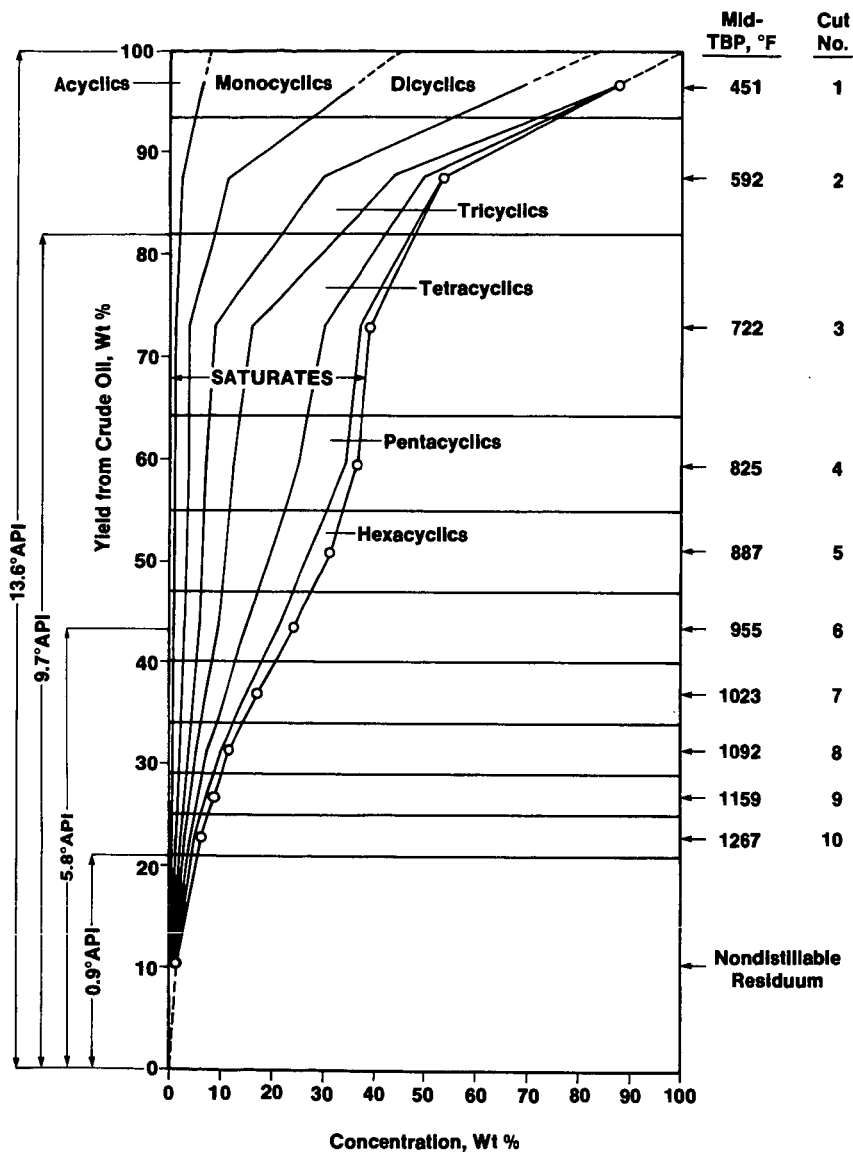
STRUCTURES OF LIQUID-LIKE SYSTEMS:
X-RAY DIFFRACTION OF MODEL ORGANIC HYDROCARBONS.

Lawrence B. Ebert, Joseph C. Scanlon, and Daniel R. Mills
Exxon Corporate Research Labs
Route 22 East
Annandale, New Jersey 08801

Introduction

Since the work of T. F. Yen in 1961 (1), there has been much
effort in the determination of the structure of petroleum
heavy ends.   Although x-ray diffraction shows broad lines,
indicative of correlation lengths of ~ 10-30 A, the d values
of the peaks have been associated with specific organic
functionality: 4.5-4.8 A (aliphatic), 3.4-3.8 (aromatic
stacking), and 2.1 A (aromatic diameter).

In two previous papers (2,3), we have performed x-ray
diffraction on the liquid phases of model organic hydrocar-
bons to obtain additional insights into these assignments.
In contrast to earlier work (1), we found that the "γ-band"
at 4.6 A was related to intermolecular interference among
paraffins, but not to interference among naphthenes, which
we found to appear at 5.3 to 5.4 A (2,3). Although the
"(002) band" at 3.4 to 3.6 A presumably does arise from the
approximately   parallel   stacking   of planar   aromatic
molecules, we found evidence for (00L) peaks at lower values
of 2Θ, arising from the small stack height of the aromatic
clusters.   The true identity period became the stack height
itself, thereby giving rise to lines at "d value" greater
than that of the "(002) band." The above inferences indi-
cated that the x-ray diffraction-based method of determining
fractional aromaticity, by comparing areas of the γ-band and
(002) band, fails for a number of reasons.

In the present paper, we extend our work on the x-ray
diffraction of liquid-phase organic hydrocarbons. Analysis
of the patterns of the methyl-branched paraffins pristane
and phytol shows an intermolecular interference maximum at
4.7 to 4.8 A, slightly higher than that found for
n-paraffins, but significantly lower than that found for
naphthenes. Diffraction of quinoline shows two (00L) peaks,
exactly the behavior exhibited by 1-methyl naphthalene
(2,3). When a given molecule contains both sp² and sp³
hybridized carbon, as in tetralin or tetrahydroquinoline,
broadening of the lines results, although when one carbon
type predominates (as in n-heptadecyl benzene), that carbon
type will dominate the diffraction pattern.

1

Experimental details

Diffraction experiments on liquids were carried out as described previously (2,3). A cell with Be windows was mounted on a Siemens Type F diffractometer, equipped with a divergent 1° slit and a receiving 0.1° slit. Copper radiation was used.

Quinoline (99%) was obtained from Aldrich. The methyl branched paraffins pristane (2,6,10,14 tetramethyl pentadecane, 99%) and phytol (3,7,11,15 tetramethyl-2-hexadecen-1-ol, 70%) were obtained respectively from Wiley Organics and Aldrich. The purity of the quinoline and pristane was verified by GC/MS; the MS pattern of the major component of the phytol showed peaks at m/e of 71 ($I=100$), 55 ($I=56$), 57 ($I=52$), and 81 ($I=33$), with the highest detected $m/e=278$, reflecting a loss of water from the pure phytol (molecular weight = 296.5). A high resolution C-13 NMR pattern of the pristane showed resonances at 19.8 δ (the methyl groups on the 6 and 10 carbons), 22.7 δ (the four equivalent "terminal" methyl groups), 24.6 δ (the central, 8, methylene carbon), 24.9 δ (the 4 and 12 methylene carbons), 28.1δ (the 2 and 14 methylene carbons), 32.9 δ (the 6 and 10 methylene carbons), 37.5 δ (the 7 and 9 methylene carbons), and 39.5 δ (the 3 and 13 methylene carbons). The reader should note that the spectrum of this isoprenoid carbon skeleton is quite distinct from that of an n-paraffin (e.g., internal methylenes at 29.8 δ, terminal methyl groups at 14.2 δ). The remarkable finding reported here is that branched paraffins and normal paraffins show different patterns in liquid-phase x-ray diffraction, because of differences in **intermolecular** packing.

Results and Discussion

The diffraction patterns of the liquids pristane, phytol, and quinoline are given in Figure 1. The "d value" of the single observed interference maximum is 4.8 A for pristane and 4.7 A for phytol, measureably higher than the 4.6 A that we have found for n-paraffins. This increase is presumably related to the presence of the methyl groups, and confirms the identification of the "γ-band" as an intermolecular interference peak of paraffins (2,3).

In contrast to the paraffins, the diffraction pattern of liquid quinoline contains two peaks in the region 10 - 45° 2θ. The larger peak is at 3.9 A, with a shoulder at 5.1 to 5.4 A. This behavior is analogous to that previously reported for 1-methyl naphthalene, and confirms our suggestion of the presence of high d value (00L) lines in aromatic clusters of stack height 15 - 25 A (2,3).

2

To see the origin of these lines, one may make an analogy between aromatic clusters and the intramolecular order of n-paraffins. In the infinite n-paraffin, polyethylene, the fundamental intramolecular repeat distance is that between the first and third carbons, a distance of about 2.5 A. As one goes to finite-sized n-paraffins, as $n-C_{18}$ or $n-C_{24}$, the fundamental intramolecular repeat distance is the length of the paraffin, and one observes a family of high d value lines obeying the relation $d(L)=$ constant/(L), in which the constant is either the length of the paraffin or twice the length of the paraffin (2,3). Exactly the same situation exists for our aromatic clusters. For the infinite aromatic stack, graphite, the fundamental stacking repeat distance in an ABAB... arrangement is the AB distance, which is 6.7 A in graphite, and the most intense observed line is the (002) at 3.35 A. As one goes to clusters of small stack height, one can observe lines obeying the relation $d(L)$ = constant/(L), just as in the case of intramolecular order of paraffins. If one insists on indexing the line near 3.4 to 3.6 A as a "(002)" line, one finds that the values of L for the other lines can be either integers or rational numbers (2,3).

In the diffraction of liquids, the major peaks observed are those arising from intermolecular interference. In the case of paraffins, the single peak observed is the γ-band, arising from interference between approximately parallel paraffin groupings. Ironically, although most discussions of the γ-band occur in the context of petroleum materials, the γ-band obtained its name from a study of coal materials (4). Of course, most coals show a dominant (002) band, arising from the intermolecular interference between aromatic molecules (5).

X-ray diffraction can, of course, be used for liquids more complex than simple paraffins or aromatics. The narrowest diffraction lines, representing the longest correlation lengths, seem to occur with spherically symmetric molecules, such as 1, 3 di-methyl adamantane (2,3) or (+)-longifolene (Aldrich 23,517-2), whose pattern is given in Figure 2. The one dimensional order of aromatic stacking can be seen even for the single ring compound, hexafluoro benzene, as seen in Figure 2. Here, the scattered intensity is increased relative to that of benzene by virtue of the fluorine atoms which are co-planar with the carbon atoms. This "assistance" does not extend to perfluoro decalin, in which case the scattering arising from carbon-carbon, carbon-fluorine, and fluorine-fluorine intermolecular distances is more complex.

What happens when one has molecules containing both sp^2 and sp^3-hybridized carbon? In tetralin, with six aromatic

3

and four aliphatic carbons, one observes only a broad dif-
fraction envelope, but in n-heptadecyl benzene (six
aromatic, seventeen aliphatic) one sees a γ-band much as in
liquid n-paraffins (3).

To more systematically study these mixed systems, we
have performed reductive alkylation on model aromatic hydro-
carbons (6). In the case of perylene, for which we found a
potassium consumption of two moles K per mole perylene (7),
we quenched with methyl iodide (CD₃I) and actually obtained
a crystalline product of di-methyl di-hydro perylene, as
illustrated in Figure 3. GC/MS analysis of this product
showed 72% to be a single isomer of di-methyl di-hydro
perylene (parent peak m/e = 288.2), with perylene itself, a
second isomer of di-methyl di-hydro perylene, and a small
amount of tri-methyl di-hydro perylene also present. It is
likely that the crystallinity of our product is correlated
with the dominance of one isomer of di-methyl di-hydro
perylene.

References

(1). T. F. Yen, J. G. Erdman, and S. S. Pollack, Anal.
Chem., 33, 1587 (1961).

(2). L. B. Ebert, J. C. Scanlon, and D. R. Mills,
Preprints, Petroleum Division of the American Chemical Soci-
ety, 28, 1353 (1983).

(3). L. B. Ebert, J. C. Scanlon, and D. R. Mills, Liq.
Fuels Tech., 2,, 257 (1984).

(4). H. E. Blayden, J. Gibson, and H. L. Riley, Proceedings
of the Conference on the Ultra-fine Structure of Coals and
Carbons, p. 176 (1944).

(5). P. B. Hirsch, Proc. Roy. Soc. A, 226, 143 (1954).

(6). L. B. Ebert, "Reductive Chemistry of Aromatic Hydro-
carbons," in Chemistry of Engine Combustion Deposits, pp.
303-376, Plenum, 1985.

(7). L. B. Ebert, submitted to Fuel, April, 1985.

4

386

PRISTANE

D = 4.8 A
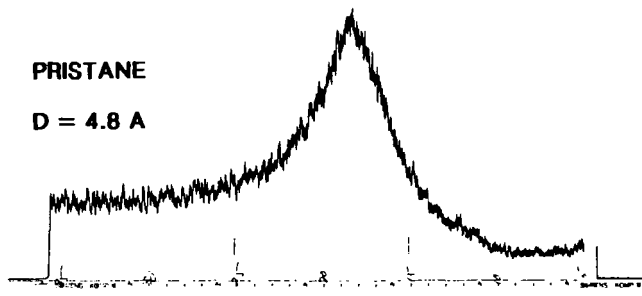
PHYTOL
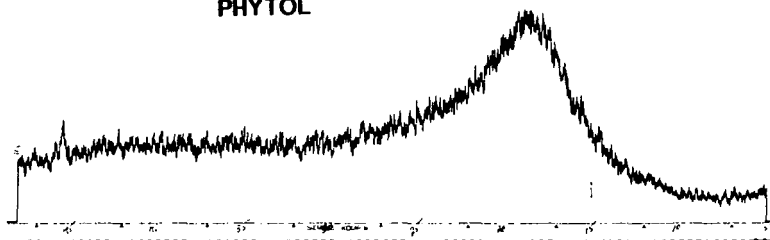
QUINOLINE

NOTE THE PRESENCE OF TWO PEAKS
AT 3.9 AND 5.1 A

25   15   DEG 2Θ (CU)
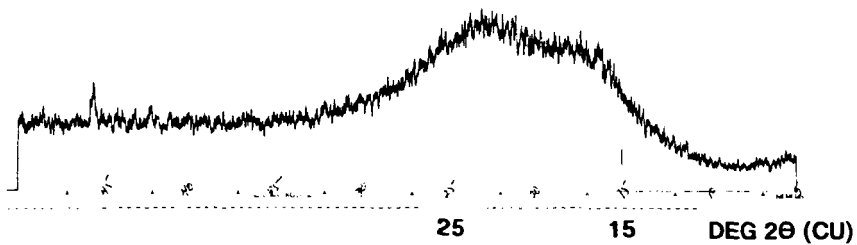
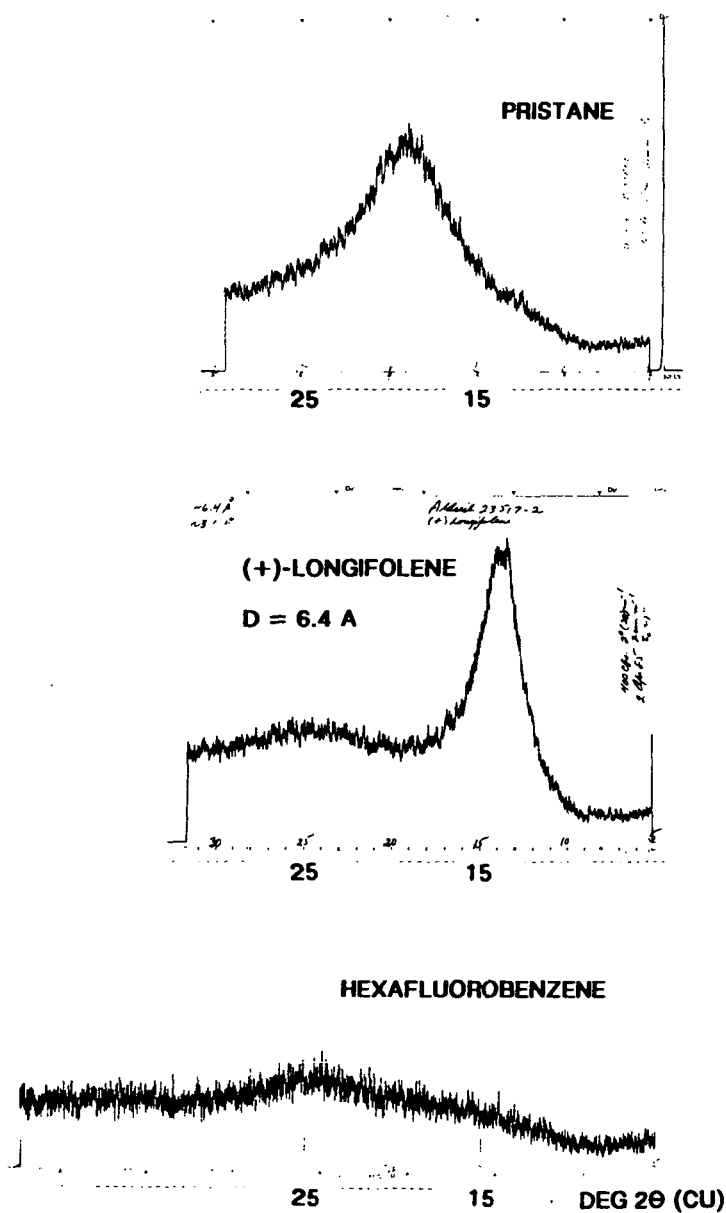FIGURE 1. XRD OF LIQUIDS.

387
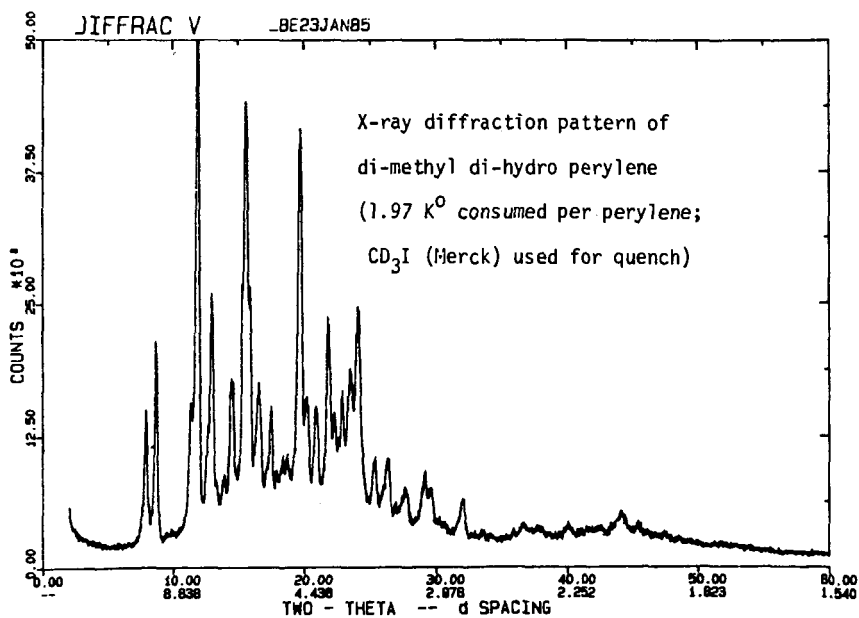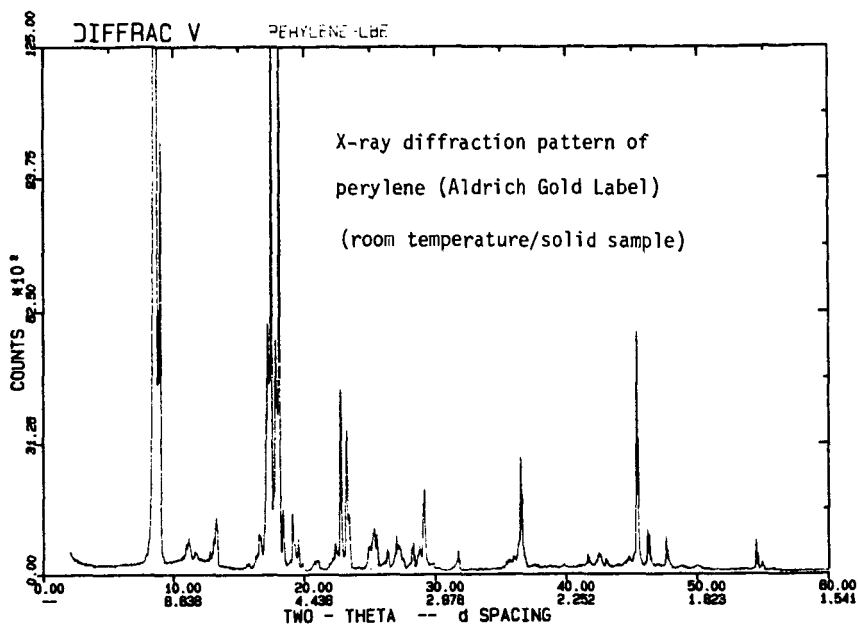
FIGURE 2. XRD OF LIQUIDS.

FIGURE 3. XRD OF PERYLENE PRODUCT.

389

REACTIONS OF HYDROGEN DURING HYDROPROLYSIS
PROCESSING OF HEAVY ENDS

by

James W. Bunger
Department of Fuels Engineering
University of Utah
Salt Lake City, Utah 84112-1183

INTRODUCTION

When heavy oils are subjected to pyrolysis in the presence of hydrogen, cracking to lower molecular weight compounds is accelerated and production of coke is inhibited compared to the case in which an inert atmosphere is present.[1-3] It has previously been reported that at very high hydrogen concentrations ($>10^3$ vol/vol) production of coke is virtually eliminated.[4] Others have reported that the presence of hydrogen improves liquid hydrogen yield when cracking residual oils.[5]

In the course of our investigations considerable attention has been given to changes in molecular structure and product characteristics. By comparing results with those obtained in the absence of hydrogen an understanding of the reactions of hydrogen is beginning to emerge. In this paper, an attempt is made to categorize the major reactions of hydrogen and to justify these reactions in terms of the observations made.

Chemical Effects Observed in Hydropyrolysis

Reduction of Coke Formation

The most obvious and perhaps most important effect of hydrogen is the inhibition of coke forming reactions. In hydropyrolysis of tar sand bitumen, which yields 16-20% coke in delayed coking processes, conditions exist in which virtually no coke is produced.[2-4] Representative results are shown in Table 1.

Table 1

Product Yields from Coking and
Hydropyrolysis of Tar Sand Bitumen

	SUNNYSIDE BITUMEN		ATHABASCA BITUMEN	
	Coking	Hydropyrolysis (Coiled Tube)	Coking	Hydropyrolysis (Verticle Tube)
		WEIGHT PERCENT YIELDS		
Gas	8.9	27.0	7.5	1.7
Liquid	71.0	73.0	76.5	93.7
Coke	20.1	NIL	16.0	4.6

When model compounds are subjected to hydropyrolysis there is no evidence for products of higher molecular weight than the starting material.[2-6] Thus, addition and condensation reactions are completely inhibited. The chemistry of coke forming reactions and the inhibition of these reactions during hydropyrolysis are discussed in greater detail in a companion paper.[7]

Reduction of Dehydrogenation of Naphthenes

It has also been observed that during hydropyrolysis little change in total aromatic carbon occurs (C_a = .22 for products and .19 for feedstock) while coking dramatically increases the aromatic carbon (C_a = .30).[8] It has also been observed that hydropyrolysis products possess a higher fraction aromatics and lower content of diaromatics than do coker products[3] (see Table 2).

Table 2

Compound Type Analysis of Total Products*
From Asphalt Ridge Bitumen

	Coking	Hydropyrolysis
Saturates	52.4	59.4
Monoaromatics	8.4	12.0
Diaromatics	6.1	4.4
Poly-Polar Aromatics	33.0	24.1
Gas/Liquid/Coke (weight percent)	4/81/15	17/83/0
Avg. M.W. Liquids	321	336

*Values given are on a feed basis; gas production is lumped into the saturates portion and coke production is lumped into the poly-polar aromatics fraction.

From the data above it is not possible to tell whether the principal effect of hydropyrolysis is to inhibit the denydrogenation of naphthenes to form aromatics or that hydrogenation of condensed aromatics to form monoaromatics is occuring. As will be shown below both appear to be happening. NMR data taken on an Athabasca bitumen and the liquid products from hydropyrolysis (93% yields) suggests that the fraction of monoaromatic carbon increases with hydropyrolysis processing. For the Athabasca case the fraction aromatic carbon (fa) declines from 0.35 t 0.28 while the fraction aromatic hydrogen (H_a) increases from .04 to .05, clearly showing lower levels condensation and/or a lower degree of alkyl substitution.

Hydrogenation of Aromatics and Olefins

The observation that total aromatic carbon remaines virtually constant (or in some cases declines) while the distribution shifts from polycondensed aromatics toward monaromatics strongly suggests that polycondensed aromatics are being hydrogenated. In hydropyrolysis where coke formation is small the amount of polyaromatics in the feed that can be accounted for by loss to coke is limited.

In an attempt to ascertain whether or not aromatics are in fact being hydrogenated during hydropyrolysis, a mixture of 5% naphthalene in n-hexadecane was hydropyrolyzed at 540°C and 2000 psig H_2 and 30 sec residence time. Approximately 6% of the naphthalene was converted to tetralin. The identity of tetralin was confirmed by mass spectroscopy. Calculations of the thermodynamic equilibrium between saturates and aromatics reveal that only the mono-aromatics are strongly favored at these conditions. In the tetralin-naphthalene system and at the reaction conditions given the equilibrium concentration for tetralin is 0.3 mole fraction (in the absence of cracking of tetralin).

As with aromatics there is also a strong tendency to hydrogenate olefins. It has previously been reported[1,2] that olefins content is reduced in hydropyrolysis by as much as 50-80% compared to thermal cracking in an inert atmosphere. At higher pressure Z 2000 psig H_2 terminal olefins are virtually absent from the products of hydropyrolysis of n-hexadecane. It is noteworthy that in the experiment in which naphthalene was added to n-hexadecane the C_5-C_{15} paraffins to olefin ration declined to 3.0 compared to 5.7 for the case when n-hexadecane was hydropyrolyzed in the absence of naphthalene. This data suggests that aromatics compete with olefins for available hydrogen during saturation.

An interesting effect of the presence of naphthalene was to reduce the conversion of n-hexadecane at constant reaction conditions. When other unsaturated bonds such as olefin, carbonyl, or sulfoxide are added to the system a similar reduction in the level of cracking of n-hexadecane is observed[11]. Also, the greater the concentration of unsaturated bonds added, the greater is the production of olefins from n-hexadecane. This inverse relationship between concentration of unsaturated species and cracking rates of saturated species clearly suggests the existence of competitive reactions.

Promotion of Dealkylation

Hydropyrolysis appears to promote dealkylation reactions. Evidence for dealkylation at the ring can be seen from NMR data for the Athabasca case in which the fraction of aliphatic hydrogen alpha to an aromatic ring is reduced from 0.27 to 0.21. In coking, by contrast, dealkylation at the benzylic position is generally favored and the fraction of aliphatic hydrogen alpha to the ring tends to increase. Further, when pentane soluble maltenes from tar sand bitumen are subjected to hydropyrolysis the products are shown to contain 11% pentane-insoluble material.[8] This material is characterized as highly dealkylated material (H/C Z 0.9).

In an attempt to examine the chemistry of dealkylation, a mixture of 20% n-propyl benzene in n-hexadecane was subjected to hydropyrolysis at 2000 psig, 540° and 30 sec residence time. In order to separate the hydrogen pressure effects from the total pressure effects a second run was made with a partial pressure of 500 psi H_2 and 1500 psi He. Reaction conditions were otherwise identical. Results are shown in Table 3. As the concentration of aromatics is increased or the partial pressure of hydrogen is decreased, the level of conversion of both reactants is decreased. These results are consistent with those stated above, which shows that hydrogen accelerates the cracking reactions.

392

The results show that dealkylation at the ring position is promoted by the presence of hydrogen. The ratio of benzene to toluene varies directly with the partial pressure of hydrogen. These results are consistent with hydrodealkylation chemistry in which attack by a hydrogen atom at an ipso position results in cleavage of the alkyl-aromatic bond.

The pressure of aromatic to the system reduces the level of olefin saturation but not as much as a reduction in the partial pressure of hydrogen. These results are consistent with those obtained when naphthalene was added to the system. Thus, the aromatic ring appears to act as a sink to deplete the population of H· in the reaction zone.

Hydropyrolysis Promotes a Broader Distribution of Products

The reduction in the C_4/C_1 ratio seen in Table 3 is consistent with an increasing thermal effect and decreasing hydropyrolytic effect. It is noteworthy that in hydropyrolysis C_3-C_4 gas production is enhanced while methane production is greatly reduced in relationship to coking[3] (at constant conversion). Further, the boiling point distribution of hydropyrolyzate is broader than with coker distillate from the same feed.[4] This is illustrated in Figure-1 which also compares the boiling point distribution of hydropyrolysis products with virgin crude oil. These results suggest that hydrogen plays on important role in free radical transfer (propogation) reactions resulting in a wider variety of cracking events than is the case with coking.
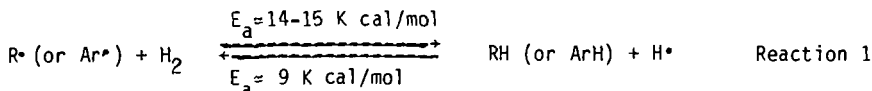
Table 3

Hydropyrolysis of n-Propylbenzene in n-Hexadecane

	Feedstock (Atmosphere)		
	n-hexadecane (H_2)	20% n-propyl benzene in $n-C_{16}$ (H_2)	20% n-propyl benzene in $n-C_{16}$ ($.25H_2$, $.75H_e$)
Conversion			
n-hexadecane	88.5	83.6	79.4
n-propyl benzene	---	31.0	26.6
Product	Product Yield (percent of n-propyl benzene converted)		
benzene	0	13.7	8.9
toluene	0	14.7	16.6
styrene	0	12.7	6.4
ethylbenzene	0	52.8	52.4
(unidentified	100	6.1	15.7
or not listed)	100	100.0	100.0
	Other Indicators		
C_8 Paraffin/Olefin	4.3	3.2	0.9
C_4/C_1	2.1	1.9	1.5

Reactions of Hydrogen

Molecular Hydrogen - The principal reaction of molecular hydrogen is as a reactant in the general metathesis reaction [1] (activation energies given are for the alkyl radical):

$$E_a = 14\text{-}15 \text{ K cal/mol}$$

$$\text{R} \cdot \text{ (or Ar} \cdot \text{)} + \text{H}_2 \quad \underset{E_a \simeq 9 \text{ K cal/mol}}{\overset{}{\rightleftharpoons}} \quad \text{RH (or ArH)} + \text{H} \cdot \qquad \text{Reaction 1}$$

The significance of this reaction to hydropyrolysis cannot be overstated. It is through this reaction that free radicals are saturated. Equally important is the fact that hydrogen atoms are produced. Production of hydrogen atoms is critical to hydropyrolysis chemistry and the mechanism shown in the above reaction provides a means for production of hydrogen atoms at modest temperatures. Good contact between hydrogen and the free radicals, is important and homogeneous, vapor-phase reaction conditions favor this reaction. Hydrogen abstraction reactions are thought to occur at appreciable rates for alkyl hydrogen at 410° and for aromatics at about 425°C during coking.[7] On this basis and considering relative bond dissociation energies, it may be predictd that the forward metathesis reaction accurs at significant rates at temperatures above about 435°C. Indeed many hydrovisbreaking processes operate at temperture regimes just above this temperature [9] and the metathesis reaction is probably important to these processes as well.

The effect of the metathesis reaction can be seen in the observations listed above. First, dehydrogenation of naphthenes is reduced because molecular hydrogen serves the function of providing hydrogen to satuarate free radicals. Second, aryl free radicals are saturated before they can add to arenes forming thermodynamically stable aryl-aryl bonds. The reaction of aryl radicals with arenes is thought to be an elementary step in coke formation[7] and suppression of coke is due in part to reaction-1. Third, alkyl radicals are saturated before they can undergo β-scission and overcrack. There is actually a reverse arguement to this latter point in which the reverse of reaction-1 results in accelerated cracking. The net effect is that molecular and atomic hydrogen act, in effect, as vehicles for the transfer of free radical resulting in a more random point of cracking than is experienced with thermal cracking. Thermal cracking is more energetically controlled and as a result the products tend to be more selectively distributed between very light gases or heavy gas oils. In hydropyrolysis, significant amounts of LPG and middle distillate are generated as discussed above.

Atomic Hydrogen

Evidence for the presence of atomic hydrogen in hydropyrolysis is clear from the observations presented. Based on reaction-1, the population of hydrogen atoms would tend to increase as the overall population of free radicals increases and as the concentration of hydrogen (gas/oil ratio) increases. Reactions of atomic hydrogen can be grouped into two general types: (i) free radical hydrogen addition and (ii) free radical hydrogen abstraction reactions.

The hydrogen addition reactions are characterized by attack on unsaturated bonds, olefins and aromatics, to form alkyl or cyclohexadienyl-type radicals, respectively. These radicals subsequently undergo metathesis

reactions with hydrogen to saturate the radical and regenerate the hydrogen atom. The presence of unsaturated bonds tends to decrease the overall population of H• as evidenced by the reduced cracking rates for n-hexadecane when unsaturated bonds are present.

If hydrogen adds to a substituted aromatic carbon it is probable that ring dealkylation will occur due to the relative strength of the C-H bond vs. the C-C bond. The same effect is not true for aryl-aryl bonds however, which are thought to be stronger than the corresponding C-H bond.[10] If hydrogen adds to an unsubstituted aromatic carbon and a hydrogen is eliminated before the free radical can be hydrogenated an unproductive event occurs which cannot be observed in the products. This reaction may, however, account for the sink for H• observed when aromatics are present.

Hydrogen abstraction reactions are also important to hydropyrolysis results. Hydrogen abstraction, or the reverse of reaction-1, results in a free radical which can subsequently undergo β-scission to crack the molecule in two. The fact that the rate of cracking of n-hexadecane depends upon the H• concentration testifies to the importance of this reaction. The broad distribution of the products as well as the relatively high concentration of LPG range gases indicates that a less selective and more random cracking is occurring. This is probably due to the less discriminating nature of H• abstraction vs. free radical abstraction in the absence of hydrogen.

SUMMARY

In summary, both molecular hydrogen and atomic hydrogen are reactants in hydropyrolysis of residual oil. The reactions of hydrogen postulated can account for the major differences between pyrolysis in an inert atmosphere and hydropyrolysis. Coke is inhibited through saturation of aryl radicals by molecular hydrogen and through hydrogenation of vinyl aromatics (and olefins) by addition of H•. Cracking rates are enhanced through hydrogen abstraction reactions. Product distribution is broadened through less energetically discriminating free radical formation. Hydrogen also seems to act as an effective heat transfer fluid and as a diluant to inhibit bimolecular addition or condensation reactions relative to unimolecular cracking reactions. In time, as the relative kinetics of these reactions become better understood specific process development routes may become apparent. The appliciblity of hydropyrolysis to upgrading feedstocks from a variety of sources and compositions should likewise become more apparent.

References

1. J. S. Shabtai, R. Ramakrishnan, A. G. Oblad, "Thermal Hydrocarbon Chemistry," Adv. Chem. Ser., 183, 297-328, (1979).

2. R. Ramakrishnan, "Hydropyrolysis of Coal Derived liquid and Related Model Compounds," Ph.D. dissertation, University of Utah, 1978.

3. J. W. Bunger, "Processing Utah Tar Sand Bitumen," Ph.D. dissertation, University of Utah, 1978.

4. J. W. Bunger, D. E. Cogswell, R. E. Wood and A. G. Oblad, "Hydropyrolysis: The Potential for Primary Upgrading of Tar Sand Bitumen," Chpt. 25, Oil Shale, Tar Sands and Related Materials, H. C. Stauffer, Ed., Adv. in Chem. Ser. 163, Amer. Chem Soc., (1981) 369-380.

5. B. Schuetze and H. Hofmann, "How to Upgrade Heavy Feeds, Hydrocarbon Processing 63, (2), 75-82, (1984).

6. U.S. Patent # 4,298,457, Nov 3, 1981.

7. J. W. Bunger, "Inhibition of Coke Forming Reactions in Hydropyrolysis of Residual Oils," submitted to Preprints, Div. of Petro. Chem. and Preprints Div. of Fuel Chem. for publication in the procedings of the National Meeting of the Amer. Chem. Soc., Chicago, Sept. 8-13, 1985.

8. J. W. Bunger and D. E. Cogswell, "Characteristics of Tar Sand Bitumen Asphaltenes as Studied by Conversion of Bitumen by Hydropyrolysis," Chpt. 13, Chemistry of Asphaltenes Adv. in Chem., Series 195, Amer. Chem. Soc., 219-236 (1981), J. W. Bunger, N. C. Li, Eds.

9. J. W. Bunger and G. Neff, unpublished data, University of Utah, 1984.

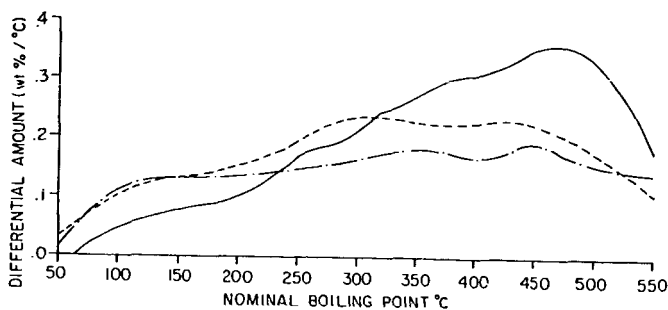10. M. Szwarc, "Energy Value for the Central C-C Bond in Diphenyl," Nature 161, 890 (1948).

Figure 1. Distillation curves for selected tar sand products and Wilmington crude oil: Asphalt Ridge coker distillate (97% distillable, 27° API) (———); Asphalt Ridge hydropyrolysis condensables (85% distillable, 25° API) (– – –); Wilmington, CA crude oil (65% distillable, 20° API) (– · –).

HYDROGEN INCORPORATION IN RESIDUUM CONVERSION

Samil Beret and John G. Reynolds

Chevron Research Company, Richmond, California   94802-0627

Introduction

In the last ten years there has been a large increase in
residuum hydroconversion capacity in the United States and overseas.
This expansion was derived from the expectation that the spread in
market values between the high sulfur fuel oil and the light transpor-
tation fuels would increase to support the large investments required
for these conversion facilities.

The reason for residuum conversion is simple--increasing the
hydrogen-to-carbon ratio (H/C) and lowering the molecular weight gen-
erates marketable distillate products. Figure 1 illustrates this
qualitatively. It shows a Stangeland (1) chart for pure paraffins,
aromatics, and a number of petroleum fractions. The residuum is
located to the right at higher carbon numbers. From a knowledge of
the boiling points of pure paraffins and polycyclic aromatics, extra
guidelines are drawn to represent approximate boiling points. This
chart is very useful because it shows the extent to which carbon
number must be reduced or hydrogen added to generate the desired light
stocks. To correct this hydrogen imbalance, various residuum con-
version processes either add hydrogen or reject carbon. A partial
list of conventional residuum conversion options is shown in Table I.
Thermal and extractive processes generally reject carbon while hydro-
conversion schemes add hydrogen.

Residuum Hydroconversion

The choice of residuum conversion process depends on the
unique set of circumstances for each refinery, for example, feed-
stocks, existing equipment, and capital constraints. If the objective
is to produce a distillate product slate, then hydroconversion can
serve as an efficient process for conversion of lower value hydro-
carbon feedstocks and heavy residuum to high quality distillate
products.

Figure 2 shows a residuum hydroconversion refinery in its
basic form is shown in Figure 2. The residuum feedstock is partially
converted to C_4-1000°F distillate liquids and C_1-C_3 gas. The hydrogen
necessary for the operation is supplied from an outside source. The
hydroconversion reaction system may be thermal, catalytic, or may
consist of a series of thermal and/or catalytic steps. Operating
conditions, nature of the catalysts, and various processing schemes

Encl. - Tables I-IV
        Figure 1 (RE 832399)
        Figures 2-6

(for example, "recycle") all affect and define the process severity. The process severity in turn affects conversion, product slate, volumetric expansion, and hydrogen consumption.

It should be noted that the operating conditions, catalysts, and processing techniques vary considerably among the commercial hydroconversion processes; but as shown in Figure 3, both the total hydrogen consumed and the residuum conversion increase invariably with increasing process severity. Figure 3 represents hydrogen consumption and conversion data for Arabian Light residuum processing at different sulfur levels (2). This representation is based on Chevron-designed catalysts operating at conditions capable of giving run lengths of at least six months. For maximum conversion, operation at high severities is required.

In this paper, we use total conversion to distillates and the hydrogen consumed by the process as relative measures of process severity. Admittedly, these are relative definitions, but they allow evaluation of hydroconversion processes in general without regard to the details unique to each process (e.g., catalyst, reactor type, temperature, etc.). For a given example, referring to Figure 3, the relative hydrogen consumed at hydrocracking conversion depends upon the desired S specification of the product. Because we are only interested in the relative hydrogen consumed, knowledge of the specific process details are not necessary.

Under the usual hydroconversion conditions (elevated temperatures and pressure, high hydrogen-to-feed ratios, and high activity catalysts), many reactions with hydrogen proceed simultaneously. These include: hydrocracking, aromatization, hydrogenation, condensation, hydrodesulfurization, hydrodenitrification, deoxygenation, demetalation, and isomerization. However, these reactions do not all occur at equal ratios. Judicious selection of catalysts and processing conditions favor one or more of these reactions over others. One can learn more about the relative impact of these reactions by studying the stoichiometry of hydrogen incorporation.

Stoichiometry of Hydrogen Reactions

We used the same analytical approach as Finseth et al. (3) in formulating the hydrogen/residuum reactions. Finseth and his colleagues were interested in coal conversion chemistry and the role of hydrogen during coal liquefaction. However, the same approach with some modifications can be used to study the role of hydrogen during residuum conversion. The fact that it is difficult to understand the molecular level mechanisms of hydrogen incorporation should not preclude understanding the overall chemistry.

As Finseth, hydrogen/residuum reactions are classified into six categories:

1. Hydrogenation and dehydrogenation.
2. Hydrocracking and (its reverse) condensation.

3. Isomerization and hydrogen exchange.
4. Desulfurization.
5. Denitrification and deoxygenation.
6. C_1-C_3 gas production.

This grouping is done basically to generalize the stoichiometries of very high number of reactions. Once the stoichiometry is established then it is possible to devise a technique which discriminates among these six hydrogen reaction routes.

We used ^{1}H and ^{13}C NMR to determine the hydrogen distribution during hydrogenation/dehydrogenation reactions. We have seen only aromatization as the dehydrogenation reactions. Hydrogenation consumes one hydrogen atom for every carbon reduced. For example, if a residuum sample containing 25 aromatic, 75 aliphatic carbons is hydrogenated to 20 aromatic, 80 aliphatic carbons, ^{13}C NMR should detect the change in aromaticity from 25% to 20%.

The second category of reactions, cracking/condensation, is more difficult to determine. No satisfactory method is available to count the number of cracking reactions occurring during residuum conversion. However, if all of hydrogen involved in the other five categories of reactions are accounted for, then we can calculate the hydrogen consumed due to cracking by difference.

The total change in hydrogen content can be determined by classical elemental analysis.

The third class of reactions, isomerization/exchange, does not affect net hydrogen incorporation. Therefore it is not considered here.

The remaining three categories are basically bond scission reactions eliminating heteroatoms and forming C_1-C_3 gases. Gas production is easily measured and analyzed with commonly available analytical instruments. Since two hydrogens are incorporated for every molecule of C_1-C_3 formed (mostly due to alkyl chain cracking reactions), these gas analyses provide a good estimate of hydrogen consumed in gas formation.

It is difficult to quantify accurately hydrogen consumed due to heteroatom (S, N, O) removal due to the multiplicity of reactions. For simplicity, we assume sulfur in the residuum occurs as thiophenic. Therefore, two hydrogen atoms are incorporated into the residuum for each sulfur removed.

We also assume nitrogen as pyrrolic and oxygen as a mixture of carboxylic and phenolic. Therefore, one hydrogen atom is incorporated into the residuum for each N or O removed.

Even though carboxylic acid amides and other compounds have been detected in residua (4), the above assumptions should not affect the calculations significantly because no residua studied contained more than 2% N, O. Furthermore, probably any deviations in

stoichiometry due to very large number of reactions involving hetero-
atoms tend to cancel each other and are therefore self-correcting.

Coking reactions produce insoluble organic material which is
not accounted for in the above analysis, primarily reducing the amount
of measurable aromaticity of the processed products. In hydroconver-
sion, these levels were all under 1%, and generally less than 0.5%.
These levels should have little affect on the calculations.

Therefore, using ^{1}H and ^{13}C NMR, as well as elemental analy-
sis and quantitative gas analysis, one can determine the net hydrogen
incorporated due to each of the six categories of reactions. Further-
more, if these determinations are coupled to process parameters, they
greatly enhance the understanding of residuum conversion chemistry and
hydrogen utilization. With these goals in mind, we conducted residuum
hydroconversion experiments at different process severities and ana-
lyzed both the liquid and gas products as well as the feed extensively
using the technique described here.

Experimental

Three California residua (designated A, B, and C) were
obtained by single-plate distillation of the corresponding crude.

The ^{13}C NMR and ^{1}H NMR spectra were recorded on either a
Bruker CXP 300 or WH-90 spectrometers. The samples were prepared as
dilute solutions in deuterated chloroform with tetramethylsilane as
reference. Integrations were performed by the spectrometers, and the
ratios were calculated by hand. The NMR spectra were interpreted by
the method of Young and Gayla (5). No olefins were observed in
spectra. Gadolinium tris(1,1,2,2,3,3-heptafluoro-7,7-dimethyl-
4,6-octanedione) was added as a relaxation agent to ensure accurate
integration of the aromatic region. The aromatic region was inte-
grated between 110-180 ppm. The aliphatic region was integrated
between 0-60 ppm. Each were calculated as percentage of the total
integrated area (minus the solvent peaks).

Total aromatic content of liquid is adjusted for the compo-
sition of the gas.

Elemental analyses were performed by Chevron Research
Company Analytical Department. C,H were done by Carlo Erba, N by
either Mettler (Dumas) or Dohrmann (ASTM D 3431), S by Dohrmann (ASTM
D 3120), and metals by either X-ray fluorescence or inductively
coupled plasma emissions. Boiling point distribution was determined
by thermogravimetric analysis (TGA). Gas composition was determined
by gas chromatography.

Hydroconversion Experiments

Hydroconversion experiments were conducted in a flow
reaction system using the heavy residua from California crudes.
Inspections of these residua are given in Table II. These residua are
very rich in nitrogen, sulfur, and metals. Arabian Heavy 730°F+ oil

is included for comparison. They represent a big challenge for the refining industry in the coming decades.

These feedstocks were processed at different severities using different sets of operating variables such as temperature, pressure, residence time, hydrogen circulation rate, and catalyst. Total hydrogen consumption varied from 600-2100 SCF/bbl of feed. Residuum conversion (1000°F+/1000°F-) ranged from 50-95%. Hydrogen consumption, 1000°F+ conversions, and the percent aromatic carbon are summarized in Table III.

Hydrogenation, Cracking, and Process Severity

The number of hydrogen atoms incorporated per 100 carbon atoms is compared in Figure 4 for Residuum A, 850°F+ cut point at three different conversion levels (Table III: Runs 2A, 2B, and 2C). With increasing process severity, the number of hydrogen atoms consumed due to cracking and gas formation reactions appears to increase linearly. The bulk of the hydrogen is used to cap the ends of cracked fragments. Since two hydrogens are incorporated for every molecule of C_1-C_3 gas formed, it is natural that hydrogen consumed in gas formation reactions also increases with increasing conversion. On the other hand, the net number of hydrogens involved in aromatic saturation remains constant in all three experiments. This may be due to all three experiments were at high levels of 1000°F+ conversion. At these high conversion levels, incremental conversion probably comes from cracking off alkyl branches from already hydrogenated species.

In Figure 5, hydrogen incorporation into Residuum A 850°F+ is compared to that of Residuum A 650°F+. As shown in Tables II and III, 850°F+ is more aromatic and contains more heteroatoms. Due to its hydrogen deficient nature relative to the 650°F+, the 850°F+ consumes more hydrogen at roughly equal process severities. Comparing Experiments 1A to 2C in Figure 5, we see that cracking reactions consume more hydrogen with 650°F+ compared to the 850°F+. With regard to hydrogenation, this order is reversed, probably because some of the hydrogen deficient species in the 850°F+ have to be hydrogenated before they crack. Due to the high conversion, the number of hydrogens involved in capping the cracked fragments far exceeds the hydrogens involved in net aromatic saturation.

In Figure 6, we compare two hydroconversion experiments conducted with Residuum B 650°F+. Experiment 3A was a thermal treatment of the feedstock, while the Experiment 3B included a catalytic treatment. The effect of these process differences is very apparent in Figure 6. The number of hydrogens incorporated due to net hydrogenation reactions is negative (-1.8/100 carbons) during Experiment 3A. This suggests that at this particular processing condition, aromatization of the residuum is occurring, and it is providing some of the hydrogen consumed for cracking and other hydrogen consuming reactions. During Experiment 3B, under different processing conditions, there is no net aromatization (indicated by the number of

hydrogens incorporated in hydrogenation). In fact, aromatic satura-
tion is the dominant reaction in this case, consuming more hydrogen
than cracking. Figure 6 is a good example of how this technique can
be used as a sensitive test of the effect of processing conditions on
different reaction pathways.

This technique also reveals the sensitivity of hydrocon-
version to characteristics of the feedstock. In Table IV, comparing
1B to 4A, total number of hydrogens incorporated is roughly the same,
24 per 100 carbons. The gross hydrogen consumption is about the same,
about 1600 SCF/bbl. However, the starting feedstocks are very differ-
ent. In Experiment 4A, the feedstock was Residuum C 950°F+, which is
very rich in aromatic carbon and hydrogen, but low in sulfur. (See
Tables II and III.) On the other hand, the feed in Experiment 1B was
Residuum A 650°F+, which is less aromatic but much higher in sulfur
(relative to Residuum C 950°F+). Due to the hydrogen deficient nature
of the Residuum C 950°F+, more of the hydrogen is consumed in hydro-
genating the aromatic species than for Residuum A 650°F+. Since over-
all conversion is the same in both experiments, there was not that
much difference in the number of hydrogens involved in cracking and
gas make. However, substantially more hydrogen was used to remove
sulfur from Residuum A 650°F+ compared to Residuum C 950°F+. There-
fore, although the same number of hydrogens were involved in both
experiments, the distribution of these hydrogen atoms were radically
different.

Conclusions

This approach yields a detailed description of hydrogen
incorporation during residuum hydroconversion. Character of the feed-
stock, processing conditions, and the catalyst all affect how hydrogen
is incorporated into residuum matrix. The two dominant reaction
routes are hydrocracking and hydrogenation.

Our data analysis suggests hydrogenation and hydrocracking
reactions incorporate hydrogen equally at moderate process severities.
At high severities, the bulk of the hydrogen is consumed by capping
reactions of cracking fragments. Judicious selection of processing
conditions favor one or the other.

The feedstock characteristics also influence hydrogen incor-
poration. With aromatic feedstocks, hydrogenation reactions compete
equally with hydrocracking for hydrogen. With less aromatic feed-
stocks, hydrocracking dominates over hydrogenation reactions.

The technique we presented here is useful in relating these
processing conditions to understanding of the overall chemistry and
exploiting these processing conditions to tailor the process and the
products to the desired product slate.

Acknowledgments

References

(1) O'Rear, D. J.; Frumkin, H. A.; Sullivan, R. F.; "Refining of Syncrudes from H-Coal Liquefaction Process," 47th Meeting of American Petroleum Institute, New York, May 1982.

(2) Bridge, A. G.; Scott, J. W.; Reed, E. M.; Oil and Gas Journal, May 19, 1975.

(3) Finseth, D. H.; Bockrath, B. C.; Cillo, D. L.; Illig, E. G.; Sprecher, R. F.; Retcofsky, H. C.; and Lett, R. G.; ACS, Div of Fuel Chem., Preprints, 28 (5), 17-25, 1983.

(4) McKay, J. F.; Harnsberger, P. M.; Erickson, R. B.; Cogswell, T. E.; and Latham, D. R.; Fuel, 60, 17-26, 1981.

(5) Young, D. C.; and Galya, L. G.; Liq. Fuels Tech.; 2 (3), 307-326, 1984.

:pgb

FIGURE 1
THE STANGELAND CHART FOR FUELS
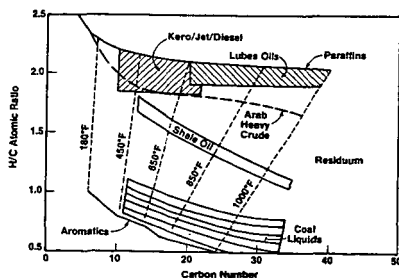
TABLE I

RESIDUUM
PROCESSING OPTIONS

Thermal Processes

. Visbreaking
. Delayed Coking
. Fluid Coking
. Steam Cracking
. Partial Oxidation

Extractive Processes

. Solvent Deasphalting

Catalytic Processes

. Residuum FCC
. Residuum Hydroconversion

TABLE II

INSPECTIONS OF FEEDSTOCKS

	Arabian Heavy	Residuum A	Residuum A	Residuum B	Residuum C
Cut Point, °F+	730	650	650	850	950
Gravity, °API	11	9.8	5	9	4.2
N, %	0.3	0.8	1.1	1.1	1.0
S, %	4.6	5.7	5.7	4.2	1.2
H, %	10.7	10.6	10.1	10.6	10.2
C, %	84.1	82.0	81.5	83.7	85.3
H/C	1.53	1.55	1.49	1.52	1.44
Ni, ppm	24	109	139	115	165
V, ppm	88	274	359	197	75
Fe, ppm	4	0	14	3	75
C_7 Asphaltenes, %	8.4	12	15	10.1	7.6
Ramscarbon, %	14	13	16.8	13.7	20.2
1000°F+ Content, %	60	48	75	46	95

4-8-85

TABLE III

HYDROCONVERSION EXPERIMENTS

Exp. No.	Identification	Total Hydrogen, % Wt	Aromatic Carbon, %	1000°F+ Conversion, %	H$_2$ Consumed, SCF/Bbl of Feed
1	Residuum A 650°F+ (Feed)	10.6	22.5	–	–
1A	(Product)	12.7	20	95	2000
1B	(Product)	12.4	20.3	84	1530
2	Residuum A 850°F+ (Feed)	10.1	26.7	–	–
2A	(Product)	12.3	20.1	79	1660
2B	(Product)	12.3	20.4	82	1750
2C	(Product)	12.4	20.3	87	2050
3	Residuum B 650°F+ (Feed)	10.5	29.5	–	–
3A	(Product)	11.2	32	60	600
3B	(Product)	11.79	22.5	73	1100
4	Residuum C 950°F+ (Feed)	10.2	33	–	–
4A	(Product)	11.9	26	77	1600

TABLE IV

HYDROCONVERSION OF
RESIDUUM C 950°F+ VERSUS RESIDUUM A 650°F+

	Residuum C 950°F+	Residuum A 650°F+
Feed		
Aromatic C, %*	33.0	22.5
Aromatic H, %**	6.7	3.2
Experiment No.	4A	1B
H Atoms Incorporated/100 C		
Due to Cracking	9.9	11.9
Due to Hydrogenation	8.3	3.0
Due to C$_1$-C$_3$	3.5	3.8
Due to Heteroatom Removal	2.4	6.0
Total	24.1	24.7

*From ^{13}C NMR.
**From ^{1}H NMR.

4-8-85

FIGURE 2

**GENERALIZED DIAGRAM
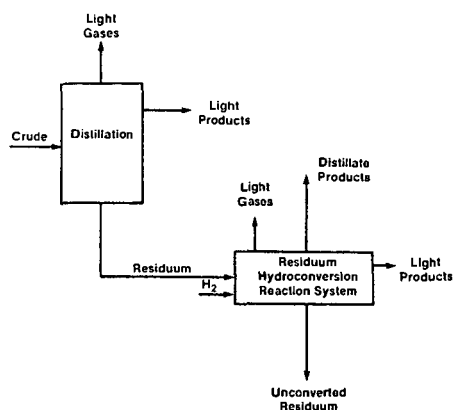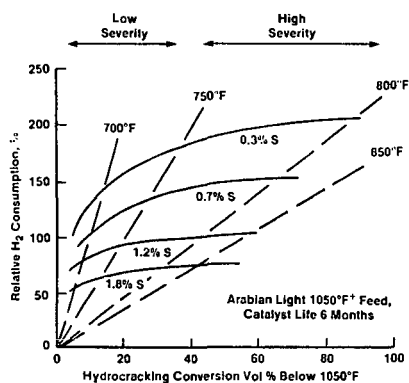RESIDUUM CONVERSION REFINERY**

FIGURE 3

H₂ USAGE IN RESIDUUM PROCESSING*

*From A. G. Bridge, J. W. Scott, E. M. Reed, The Oil and Gas J, May 19, 1975

FIGURE 4

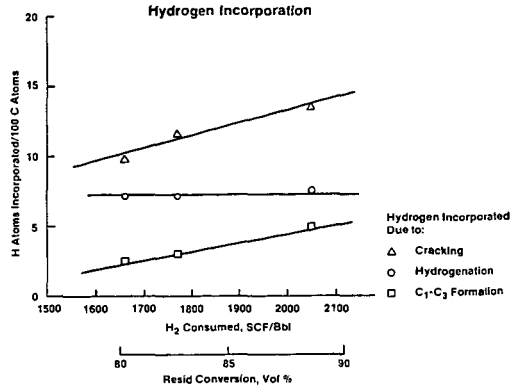HYDROCONVERSION OF RESIDUUM A 850°F⁺

Hydrogen Incorporation

FIGURE 5
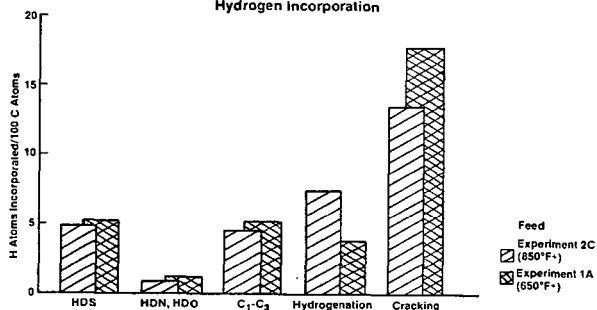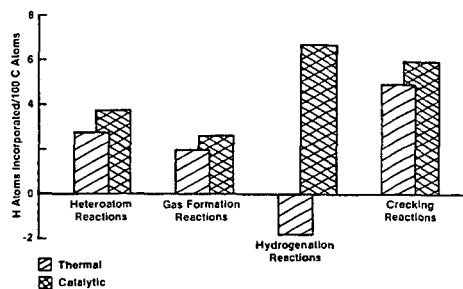
HYDROCONVERSION OF RESIDUUM A

Hydrogen Incorporation

FIGURE 6

HYDROCONVERSION OF RESIDUUM B 650°F⁺

Thermal Treatment Versus Catalytic Treatment

407

PETROLEUM ASPHALTENE THERMAL REACTION PATHWAYS

P.E. Savage, M.T. Klein, and S.G. Kukes[*]

Department of Chemical Engineering
and
Center for Catalytic Science and Technology
University of Delaware
Newark, DE 19716

[*]Research and Development Center
Phillips Petroleum Company
Bartlesville, OK 74004

INTRODUCTION

The industrial trend toward processing comparatively refractory heavy crudes and residua that can contain appreciable portions (10%-30%) of asphaltenes assures interest in their thermolysis. Most previous pyrolyses of asphaltenes have been oriented toward either elucidation of their structure (1,2) or the identification of fragmentation products and the dependence of their yields on pyrolysis temperature (3-6). Pyrolysis kinetics related to global product fractions (e.g. asphaltene, maltene, coke) have also been reported (2,7). Little information exists, however, about the variation of the yields of the individual constituents of the product fractions with both time and temperature. Further, operative thermolysis mechanisms, e.g. pericyclic or free-radical, are obscured in the complexities of the reactions of actual asphaltenes. The foregoing motivated the present investigation of the pyrolysis of both precipitated asphaltenes and an asphaltene model compound, pentadecylbenzene.

EXPERIMENTAL

The asphaltenes were isolated from an off-shore California crude oil via a standard procedure of precipitation with 40 volumes of n-heptane. Pentadecylbenzene (PDB), 99.4% by GC analysis, was obtained from Alfa Products and used as received.

Reactors

The isothermal, batch pyrolyses were at temperatures between 350°C and 450°C for times ranging from 5 to 180 minutes. Two reactors were used. The first, used in asphaltenes' thermolyses, consisted of nominal 3/8 in stainless steel capped Swagelok port connectors attached to the two ends of a union tee. A reducer connected the center port of the tee to a 12 in length of 1/4 in o.d. stainless steel tubing. A 1/4 in Whitey severe service union bonnet valve interposed in the tubing served as a shut-off valve and also allowed attachment of a gauge for measurement of pressure. The second reactor, used in model compound pyrolyses, was assembled from a nominal 1/4 in port connector and two 1/4 in caps.

Procedure

For the asphaltene thermolyses the reactors were typically loaded with 1 g of asphaltene and purged with argon. The shut-off valve was then closed, and the reactor plunged into a Tecam fluidized sandbath that had been preheated to the pyrolysis temperature. After the desired reaction time had elapsed the reactor was removed from the sandbath and immediately immersed in ice water to quench the reaction. After the reactor assembly had cooled and equilibrated at room temperature, the number of moles of gas produced during pyrolysis was estimated by measuring the reactor pressure. The gaseous products were subsequently analyzed by

gas chromatography. After removing the tubing and the shut-off valve, a small amount of phenylether was added to the reactor contents to serve as an external standard in the ensuing chromatographic analysis of the heptane-soluble products. The reaction products were next subjected to a series of solvent extractions (8) to separate and collect the pyrolysis product fractions which were subsequently analyzed gravimetrically and by GC and GC-MS.

During a typical model compound experiment, reactors were loaded with about 50 mg of PDB and then 3 mg of diphenylmethane was added to serve as an internal standard in the chromatographic analysis. After purging with argon, the reactors were sealed, immersed in the preheated sandbath, and after the desired reaction time had elapsed, removed from the sandbath and quenched in cold water. Once cool, the reaction products were collected in acetone and analyzed by GC.

RESULTS AND DISCUSSION

Asphaltene Thermolysis

Asphaltene pyrolysis products and global kinetics are summarized in Table 1, which lists, for reactions at 350, 400 and 450 °C, respectively, holding time, product identification, product yields, and the apparent first order rate constant for asphaltene decomposition.

Pyrolyses at 350 °C yielded gas, maltene (heptane-soluble), and unreacted asphaltene (heptane-insoluble, benzene soluble) product fractions. Coke (heptane-insoluble, benzene-insoluble) did not form, and mass balance closure averaged 97%. The ultimate asphaltene conversion was less than 10%. Within the product fractions listed above, the most abundant of the individual products were the light nonhydrocarbon and hydrocarbon gases H_2S, CO_2, CH_4, C_2H_6, C_3H_8, n-C_4H_{10}, and n-C_5H_{12}. The maximum total gas yield observed was about 1.0% after 150 min. The maltene fraction yield was about 10% by weight of the original asphaltene after 150 min at this temperature. No individual product constituted a major portion of the maltene fraction but a series of n-paraffins was identified with each present in trace amounts.

Asphaltene thermolysis at 400 °C produced coke in addition to gas, maltene, and asphaltene fractions. Mass balance closure varied from 79% to 96%. Major gaseous products at 400 °C were H_2S, CH_4, C_2H_6, C_3H_8, nC_4H_{10}, and nC_5H_{12} along with lesser amounts of CO_2 and C_2H_4. The n-alkanes up to C_{26} and various cycloalkanes were the most abundant products in the maltene fraction at this temperature. The single-ring aromatics toluene and the xylenes were also detected in smaller proportions.

Figure 1a summarizes the temporal variation of the yields of pyrolysis product fractions at 400 °C. Maltenes were more abundant than gases at all times, and the nearly discontinuous rate of generation of coke at 30 min coincided with rapid asphaltene conversion. Note that during this period of apparently rapid asphaltene reaction the yields of gas and maltene did not increase dramatically.

Figure 1b shows the effect of reaction time on the yield of the major gaseous products. H_2S was once again the major product and its yield reached an asymptotic value of about 18 mg/g asphaltene after 120 min. This represents about 23% of the sulfur content of the original asphaltene.

Figure 1c depicts the temporal variations of selected n-paraffins at 400 °C. The yields of each alkane were nearly equal initially, but at longer times yield decreased as carbon number increased. Note that eicosane and tetracosane exhibit maximum yields. This behavior indicates that these alkanes underwent secondary decomposition.

Asphaltene pyrolysis at 450 °C produced gas, maltenes, coke, and unconverted asphaltene. Mass balances ranged from 60% to 74%. Asphaltene conversion, to predominantly coke, was rapid, and was complete after

30 min. The major constituents of the gaseous fraction were saturated hydrocarbons along with H_2S, and the identified maltenes included cyclopentane, methylcyclopentane, methylcyclohexane, toluene, cyclohexane, xylenes, naphthalene, and C_5 to C_{26} n-paraffins.

For pyrolysis at 450°C, the proportions of the product fractions at 90 min aligned in the descending order of coke, gas, and maltene. Within the gas fraction H_2S was a major product, and its nearly constant yield of ≈16 mg/g was of the same magnitude as the yields of methane and ethane. The yields of saturated hydrocarbon gases increased steadily with time even after 30 min where asphaltene conversion was complete. Thus in addition to primary routes from the asphaltene, light hydrocarbon gases were also produced by secondary reactions of the maltenes and/or coke.

Pyrolysis Pathways

Petroleum asphaltenes are generally considered to comprise peri-condensed aromatic units linked by aliphatic, naphthenic, or heteroatomic functionalities. The peripheries of these aromatic sheets are highly substituted by similar moieties (9-12). The present results combine with the foregoing interpretation of asphaltene structure to permit resolution of asphaltene pyrolysis pathways as well as the secondary reactions of primary products. The heteroatomic gases H_2S and CO_2 were the major primary products observed from low temperature thermolyses and likely evolved from scission of low-energy thioether and carboxylic acid moieties respectively. Higher temperature primary products that arose from fragmentation of carbon-carbon bonds were hydrocarbon gases, cycloalkanes and paraffins. It would thus be consistent that the coke observed is actually the aromatic asphaltenic core stripped of its peripheral substituents. This strictly primary product evidently transforms from benzene-soluble to benzene-insoluble over a very small "window" of degradation (see Figure 1a).

The products in the maltene fraction clearly undergo secondary reactions. This is substantiated by the maximum maltene and total paraffin yields observed at 400 and 450°C (see Table 1) which are consistent with the notion of consecutive reactions.

Figure 2 is a summary of the reaction pathways suggested above. Primary asphaltene reactions produce asphaltenic core (coke), maltenes, and gas. Secondary reactions include fission of maltenes to lower molecular weight maltenes and gases, as well as reaction of the core to gas. Note that severe overreaction of primary products is not required to predict the formation of large quantities of benzene-insoluble solid materials. This network is similar to that proposed by Schucker and Keweshan (2) and supported by Speight and Pancirov (1).

Pentadecylbenzene Thermolysis

A summary of PDB pyrolyses at 375, 400, 425, and 450°C is given in Table 2, which lists typical data concerning holding times, major products yields, product groups (i.e. homologous series) yields, and observed first-order rate constants.

Pyrolysis of pentadecylbenzene (PDB) at 400°C yielded toluene, 1-tetradecene, n-tridecane, styrene, and ethylbenzene as major products. Also appearing at the longer reaction times in lower yields were a series of n-alkanes and α-olefins containing 6 to 14 carbon atoms as well as 1-phenylalkanes and phenylolefins (α-phenylalk-ω-enes) with alkyl chains containing 2 to 12 carbon atoms. Phenylbutene was not detected. The ultimate PDB conversion was 73% at 180 minutes. The Identified Products Index (IPI), herein defined as the total weight of all identified GC-elutable products divided by the weight of PDB initially loaded in the reactor, averaged 87%. The molar balance on aromatic rings averaged 86%. Charring occurred at this temperature.

Figure 3 illustrates the temporal variations of the yields of the major products at 400°C. Toluene was the most abundant product throughout the course of the reaction. The 1-tetradecene yield followed toluene

initially, but its yield decreased after reaching a maximum value at 60 minutes. The n-tridecane yield increased steadily at this temperature. During the initial 45 minutes of reaction, the styrene yield exceeded that of ethylbenzene, but after that time its yield decreased while the ethylbenzene yield continued to increase.

PDB thermolysis at 425°C resulted in products identical to those observed at the lower temperatures. The ultimate PDB conversion was 98% after 180 minutes. The IPI averaged 70% but ranged from 98% at short times to 43% at 180 minutes. Char was observed in the reactor, so this product, along with a few unidentified products, may account for the balance of the material. The aromatic ring molar balance averaged 86%.

Table 2 shows that toluene was once more the major product. For short times of less than 15 minutes, 1-tetradecene followed toluene in abundance. The other major products aligned in the order n-tridecane, styrene, and ethylbenzene. As the reaction progressed however, the tetradecene and styrene yields decreased rapidly, and the n-tridecane yield decreased less rapidly. At 150 minutes the product alignment was toluene (50.4%), ethylbenzene (17.1%), tridecane (5.0%), styrene (0.4%), and tetradecene (0.4%).

PDB Thermolysis Pathway

A previous pyrolysis of PDB at 450°C and 600kPa by Mushrush and Hazlett (13) revealed that the major products were toluene, styrene, n-tridecane, 1-tetradecene, and ethylbenzene. They reported no kinetic constants but did explain the observed product distribution on the basis of two-step Fabuss-Smith-Satterfield theory.

The present results, in agreement with Mushrush and Hazlett, show that the major products from PDB thermolysis at low conversion were toluene, 1-tetradecene, n-tridecane, styrene, and ethylbenzene. At higher conversions, a complete series of n-alkanes, α-olefins, phenylalkanes, and phenylolefins were produced. Based on the criterion of a positive initial slope on the molar yield vs. time curve, toluene, 1-tetradecene, styrene, and n-tridecane were all primary products. Ethylbenzene was also a primary product but was produced mainly via secondary reactions. Figure 4, which shows the selectivity of PDB to to each of the major products, confirms the above assignments and also suggests that toluene and 1-tetradecene were produced through the same reaction pathway since their selectivities at zero conversion were similar. Due to the rapid secondary reactions of styrene it is difficult to determine its selectivity at zero conversion. However, it does appear to be nearly that of n-tridecane. Thus styrene and n-tridecane are likely products of the same reaction path.

These experimental observations are summarized in the thermolysis pathway of Figure 5.

Kinetic Analysis

The overall order of the reaction of PDB was determined through a series of pyrolyses at 400°C wherein the initial reactant concentration ranged from 0.0044M to 2.27M. Overall "first order" rate constants corresponding to the initial concentrations studied are presented in Table 2. The concentration dependence of these rate constants indicate that PDB thermolysis was 1.07 order.

Having determined the thermolysis of PDB to be essentially first order, overall PDB decomposition Arrhenius parameters of $E^* = 55,455$ cal/mole, $A = 1.10 \times 10^{14}$ sec^{-1} were determined.

PDB Thermolysis Mechanisms

Two possible operative PDB thermolysis mechanisms are illustrated in Figure 6 and include an intramolecular retro-ene mechanism and a free-radical chain reaction. These were both considered by Mushrush and Hazlett. The retro-ene reaction involves intramolecular hydrogen transfer to produce toluene and 1-tetradecene, whereas the free-radical reaction involves a sequence of elementary steps including initiation, hydrogen abstraction, β-scission, and termination.

Both mechanisms are consistent with the observed first order kinetics as well as the observation that toluene and 1-tetradecene initially formed in equal yields. However, the concerted mechanism alone fails to account for the formation of all observed products. In contrast, the free-radical formed from PDB via hydrogen abstraction at the α-carbon can undergo β-scission to produce styrene and n-tridecane, whereas the radical formed via hydrogen abstraction at the γ-carbon can similarly produce toluene and 1-tetradecene. Hydrogen abstraction at other positions can account for the formation of the minor products.

Rationalization of the selectivity to toluene exceeding that to styrene requires closer scrutiny. Whereas hydrogen abstraction is likely more rapid at the α-carbon (C-H bond energy $\approx$ 85 kcal/mole) (14) than the γ-carbon (ca. 95 kcal/mole) , thus suggesting formation of styrene preferably over toluene, the subsequent β-scission reaction step is more rapid for the γ-radical (C-C bond energy $\approx$ 67 kcal/mole) than the α-radical (ca. 80 kcal/mole). Clearly both of these competing effects influence the relative proportions of toluene and styrene in the products. The higher toluene selectivity observed experimentally thus indicates that the favorable energetics of the β-scission reaction outweigh the unfavorable γ-hydrogen abstraction. Note, however, that the high toluene selectivity can also be accounted for by an efficacious retro-ene mechanism occurring in parallel with a free-radical mechanism.

Implications to Asphaltene Reactivity

Plausible extension of these model compound results to asphaltene reactivity follows. The aromatic portions of petroleum asphaltenes, in contrast to PDB, contain more than a single ring. A hypothetical average structure based on 12 condensed aromatic rings has been proposed for Athabasca asphaltene (15). Furthermore, several of these large aromatic sheets are joined together in polymeric fashion by aliphatic, naphthenic, or heteroatomic linkages (9,10,12) to form an even larger asphaltene particle. Recall that to account for the high toluene selectivity of PDB, the proposed radical mechanism required that the alkylaromatic benzylic radical be an important intermediate and serve as a chain carrier. The analogous asphaltenic alkylaromatic radicals would be markedly larger and considerably less mobile than the benzylic radical. This diminished mobility will trap the radicals near their point of origin and thus constrain them to react with nearby atoms. Furthermore, at reaction conditions, asphaltene is considerably more viscous than PDB, thus further frustrating radical diffusion and transport. These likely diffusional limitations (size and viscosity), most significant at low asphaltene conversion, may increase the initial importance of intramolecular concerted reactions (e.g. retro-ene) and free-radical reactions with neighboring moieties in asphaltene relative to the model compound reactions.

CONCLUSIONS

1. Asphaltene pyrolysis includes primary reactions to its aromatic core, maltene, and gas product fractions. Components in each of these product fractions undergo secondary degradation to lighter products, gas, and presumably, char.

2. The present results indicate that the Schucker and Keweshan asphaltene structural model is a reasonable one, and that the observed yields of pyrolysis products and product fractions can be interpreted using their hypothetical average structure.

3. PDB thermolysis to toluene, styrene, n-tridecane, and 1-tetradecene as major products likely occurs by a β-scission-dominated set of radical steps, but may include a concerted component.

REFERENCES

1. Speight, J.G.; Pancirov, R.J. *Am. Chem. Soc. Div. Pet. Chem. Prepr.* **1983**, 28, 1319.

2. Schucker, R.C.; Keweshan, C.F. *Am. Chem. Soc. Div. Fuel Chem. Prepr.* **1980**, 25, 155.

3. Cotte, E.A.; Calderon, J.L. *Am. Chem. Soc. Div. Pet. Chem. Prepr.* **1981**, 26, 538.

4. Ritchie, R.G.S.; Roche, R.S.; Steedman, W. *Fuel* **1979**, 58, 523.

5. Moschopedis, S.E.; Parkash, S.; Speight, J.G. *Fuel* **1978**, 57, 431.

6. Strausz, O.P.; Jha, K.N.; Montgomery, D.S. *Fuel* **1977**, 56, 114.

7. Schucker, R.C. *Am. Chem. Soc. Div. Pet. Chem. Prepr.* **1983**, 28, 683.

8. Savage, P.E.; Klein, M.T.; Kukes, S.G. *Ind. Eng. Chem. Proc. Des. Dev.* accepted.

9. Speight, J.G.; Moschopedis, S.E. in "Chemistry of Asphaltenes" ; Bunger, J.W. and Li, N.C. Eds.; Am. Chem. Soc. Adv. Chem. Ser. **1981**, 195, 1.

10. Yen, T.F. in "Chemistry of Asphaltenes" ; Bunger, J.W. and Li, N.C., Eds.; Am. Chem. Soc. Adv. Chem. Ser. **1981**, 195, 39.

11. Yen, T.F.; Wu, W.H.; Chilingar, G.V. *Energy Sources* **1984**, 7, 275.

12. Yen. T.F. *Energy Sources* **1974**, 1, 447.

13. Mushrush, G.W.; Hazlett, R.N. *Ind. Eng. Chem. Fundam.* **1984**, 23, 288.

14. "CRC Handbook of Chemistry and Physics", 59th ed.; Weast, R.C., Ed.; CRC Press: Boca Raton, FL, 1978.

15. Speight, J.G. *Fuel* **1970**, 49, 134.

FIGURE I: ASPHALTENE THERMOLYSIS 400°C TEMPORAL VARIATIONS OF PRODUCTS
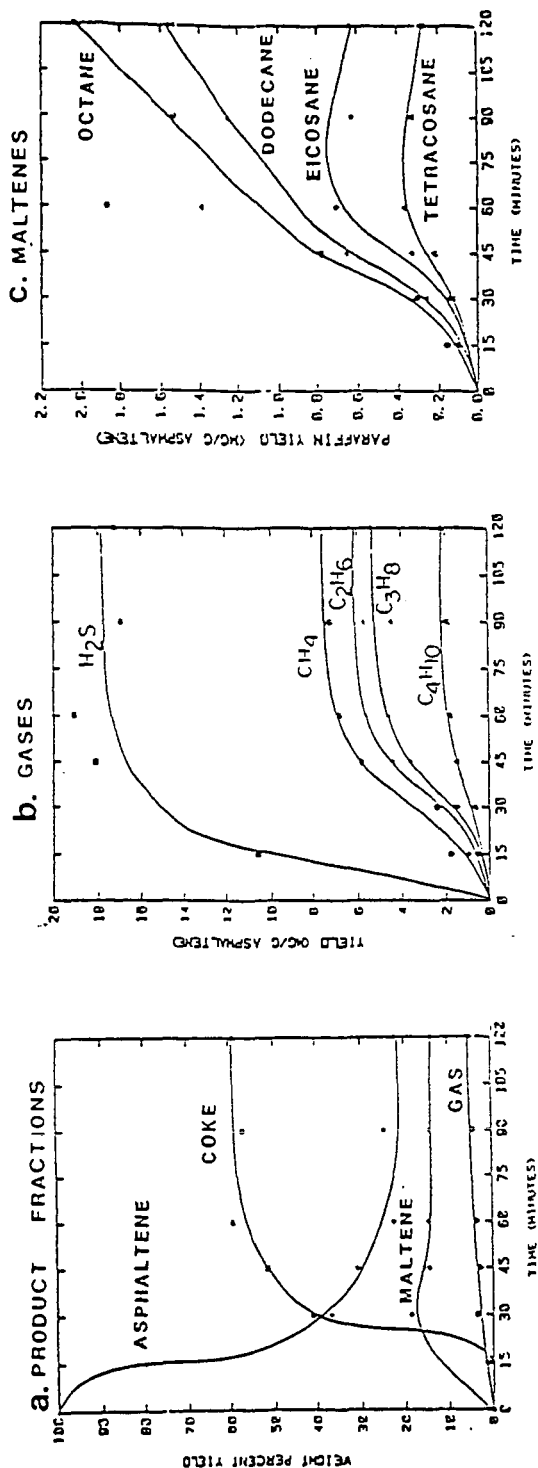
414

FIGURE 2: ASPHALTENE REACTION PATHWAYS

ASPHALTENE $\longrightarrow$ CORE   +   MALTENE   +   GAS

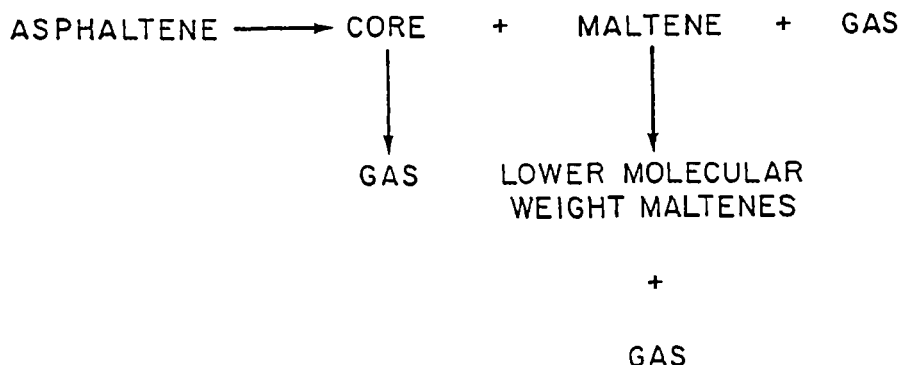GAS   LOWER MOLECULAR
WEIGHT MALTENES

+

GAS

FIGURE 3
PENTADECYLBENZENE THERMOLYSIS 400 C

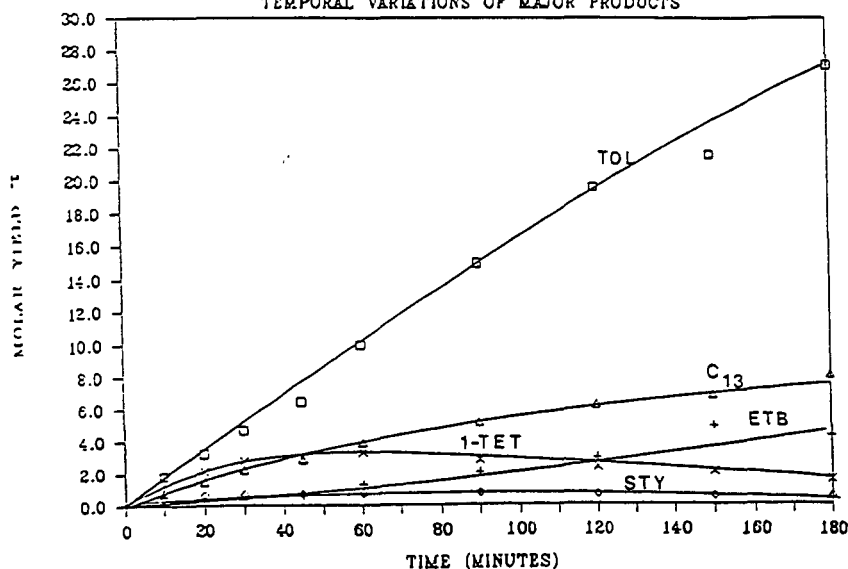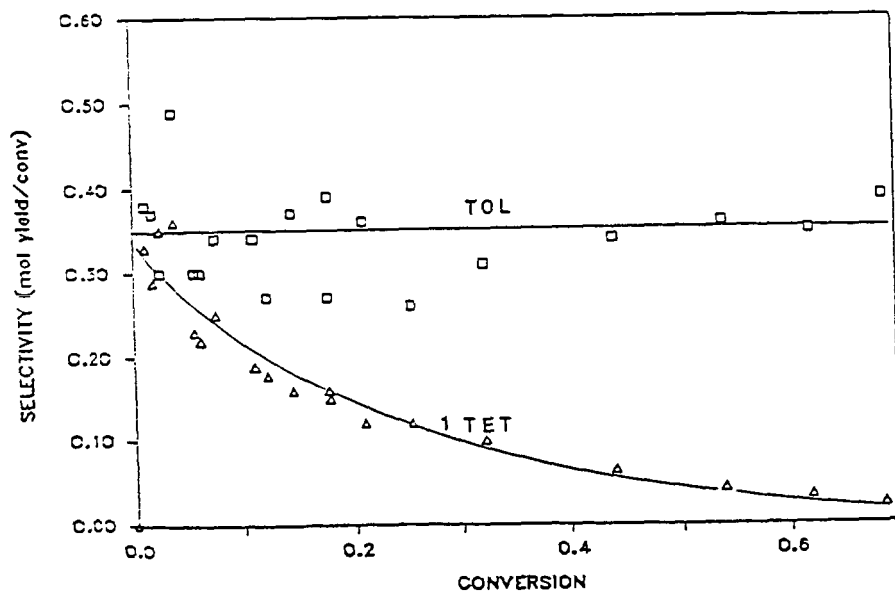TEMPORAL VARIATIONS OF MAJOR PRODUCTS

FIGURE 4:PDB SELECTIVITY TO PRODUCTS

FIGURE 5
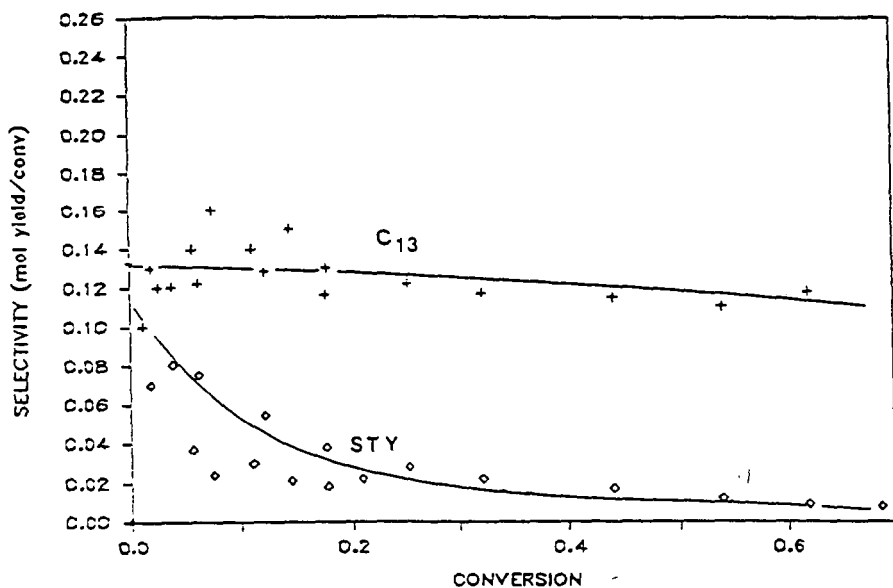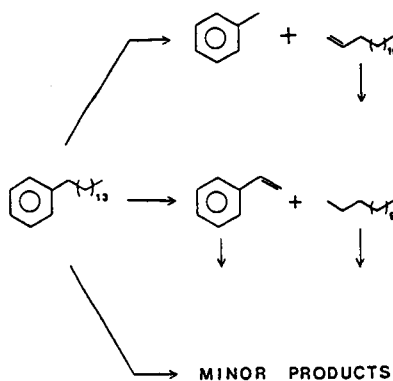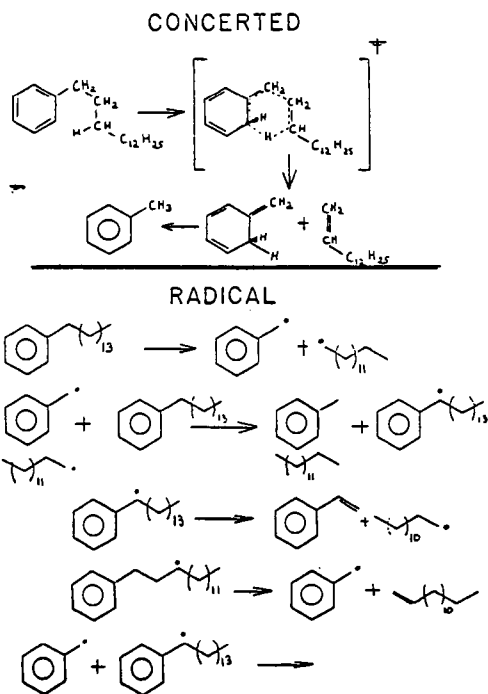## PDB THERMOLYSIS PATHWAY

FIGURE 6   PDB THERMOLYSIS MECHANISMS

CONCERTED

RADICAL

417

Table I
Asphaltene Master Table

Holding Time (min)	30	60	90	30	60	90	10	60	90
Temperature		350°C			400°C			450°C	
Product Fractions (wt%)									
Asphaltene	95.9	92.6	87.0	36.6	22.6	24.6	8.7	0	0
Maltene	4.9	6.4	8.1	18.6	14.6	14.3	12.2	9.5	10.0
Gas	0.3	0.6	0.7	3.8	3.7	4.5	6.8	12.6	14.0
Coke*	0	0	0	41.0	59.1	56.6	72.3	77.9	76.0
Mass Balance	101.1	99.3	95.8	96.3	79.0	91.8	74.0	66.2	67.2
Gas Yields (mg/g)									
H_2S	0.08	0.61	2.31	10.4	19.0	16.9	14.2	14.7	17.3
CO_2	0.06	0.61	0.69	0.93	1.29	1.18	0.97	0.90	1.23
CH_4	0.07	0.13	0.50	2.41	6.82	7.21	8.24	15.2	19.7
C_2H_6	-	0.05	0.26	1.63	5.59	5.70	6.52	13.2	16.8
C_3H_8	-	0.06	0.22	1.47	4.63	4.45	4.56	9.49	11.7
$n-C_4H_{10}$	-	0.03	0.09	0.64	1.77	1.92	2.12	3.50	4.24
C_5H_{12}	-	0.09	0.14	0.56	1.79	1.74	2.18	2.65	2.62
C_2H_4	-	0.02	0.03	0.12	0.20	0.19	0.34	0.53	0.58
n-alkane Yields (mg/g)									
$n-C_8H_{18}$	-	-	0.06	0.31	1.87	1.53	2.33	3.70	1.35
$n-C_{12}H_{26}$	-	-	0.05	0.26	1.39	1.25	1.83	2.12	0.95
$n-C_{16}H_{34}$	-	-	0.06	0.46	1.05	1.00	1.32	0.85	0.22
$n-C_{20}H_{42}$	-	-	0.07	0.15	0.71	0.63	0.74	0.23	0.07
$n-C_{24}H_{50}$	-	-	-	0.13	0.36	0.33	0.30	-	0.03
Total (C_8-C_{25})	-	-	0.8	4.4	18.4	16.8	20.9	19.5	7.0
Pseudo-First Order k(min^{-1})		0.000597			0.01227			0.24418	

*Coke yields are calculated by difference.

Table 2
PDB Master Table

Holding Time (min)	30	90	150	30	90	150	30	90	150	10	30	60
Temperature	375°C			400°C			425°C			450°C		
Product Yield (mol %)												
PDB	93.1	91.0	78.0	73.6	54.1	35.5	47.0	7.06	4.62	24.4	2.93	0.43
Toluene	1.88	3.84	6.98	4.68	15.0	21.6	18.1	47.4	50.4	20.9	47.9	64.5
1-tetradecane	1.38	2.14	2.62	2.80	2.84	2.09	3.30	0.73	0.40	3.80	0.29	0.10
n-tridecane	0.45	1.28	2.72	2.26	5.17	6.84	5.68	5.17	4.99	6.33	3.42	1.32
Styrene	0.32	0.33	0.32	0.67	0.75	0.54	1.44	0.49	0.40	2.96	0.64	0.39
Ethylbenzene	0.20	0.38	1.07	0.40	2.05	4.88	3.35	18.7	17.1	3.65	18.00	27.24
Product Group Yields (mol %)												
Phenyl-alkanes	3.01	5.44	15.2	7.96	24.8	37.4	31.3	79.8	81.3	35.7	77.0	101.5
Phenyl olefins	0.91	1.09	1.65	1.81	2.47	2.30	4.19	1.62	1.24	6.84	1.53	0.60
Alkanes	1.59	2.58	6.92	4.04	11.2	17.3	14.0	32.3	33.3	18.2	26.9	27.1
α-olefins	2.35	3.04	5.17	4.36	6.46	5.60	10.1	8.15	7.09	10.9	7.38	4.42

Pseudo-First-Order Kinetics

C_o(mol/l)	k(min^{-1})	C_o(mol/l)	k(min^{-1})	C_o(mol/l)	k(min^{-1})	C_o(mol/l)	k(min^{-1})
2.2	.00129	0.0043	.00400	2.0	.0265	1.7	0.1178
		0.0075	.00503				
		0.0150	.00535				
		0.0249	.00521				
		0.0913	.00347				
		0.482	.00452				
		1.12	.00690				
		1.80	.00783				
		2.07	.00732				
		2.29	.00690				

419

FREE RADICAL CRACKING OF HIGH MOLECULAR WEIGHT BRANCHED ALKANES

Y.V.Kissin

Gulf Research and Development Co.
P.O.Drawer 2038, Pittsburgh, PA 15230

Studies of thermocracking of branched alkanes play an important role in several areas, including high temperature catalytic cracking, delayed coking, manufacture of olefins, degradation of polymers, and geochemistry. Although principal chemical reactions involved in thermocracking under relatively mild conditions are well known (1-4), detailed information about cracking of large branched molecules is lacking from the literature, mostly because of analytical problems - identification of reaction products, various branched alkanes and olefins, in the carbon atom number range $C_8 - C_{20+}$.

This paper discusses principal reaction stages of thermocracking of pristane, phytane, and squalane in the liquid state under mild conditions ($250^{\circ}C$, 24 h) and presents analysis of reactivities of various C-H bonds in the hydrogen abstraction reactions as well as reactivities of various C-C bonds in the β-scission reactions.

EXPERIMENTAL PART

Thermocracking of pristane, phytane, and squalane at $250-300^{\circ}C$ for 24 h in the liquid state was carried out in small glass ampoules sealed under vacuum. Under these conditions the reaction yields equimolar mixtures of isoalkanes and olefins with branched chains. Addition of a mineral clay (bentonite) to the ampoules results in conversion of the olefins into a complex mixture of various secondary products while keeping the alkanes formed in the cracking reaction intact. Comparison of the gas chromatograms of the cracking products obtained with and without the clay assists in identification of branched alkanes.

A Hewlett-Packard 5880A gas chromatograph equipped with the flame ionization detector, operated in the split injection mode with a split ratio 100:1, was used to obtain chromatographic data. The column used was a 50 m, 0.02 mm i.d., fused silica capillary coated with 0.50 micron film of cross-linked methyl silicone. Helium carrier gas was used at a flow of 1 ml/min. The column oven temperature was programmed from $40^{\circ}C$ to $300^{\circ}C$ at $5^{\circ}C/min$ and held at $300^{\circ}C$ until complete elution of a sample. Sample size was 1.0 microliter. Detector and injector temperatures were held at $325^{\circ}C$. Samples were diluted with CS_2 before injection.

The techniques used for assignment of alkane and olefin peaks in gas chromatograms of the thermocracked products are discussed elsewhere (5, 6). They were based on the application of a modified additivity principle (7) which allows quantitative estimation of peak positions of complex molecules (multibranched alkanes and olefins) from the data on peak positions of more simply built molecules (monobranched alkanes, linear olefins).

A generally used procedure of presentation of retention times for peaks of hydrocarbons in gas chromatograms is calculation of their Kovats factors (KF) from their retention times RT (8).

$$KF(\text{iso-alkane } C_nH_{2n+2}) = 100(n-1) +$$

$$100[RT(\text{iso-alkane})-RT(n-C_{n-1}H_{2n})]/[RT(n-C_nH_{2n+2})-RT(n-C_{n-1}H_{2n})] \qquad 1)$$

For example, the peak of an iso-alkane situated in the middle between peaks of $n-C_{12}H_{26}$ and $n-C_{13}H_{28}$ has KF 1250. We found it more convenient to use a different parameter for the purpose – a relative retention factor, RRF (5, 6):

$$RRF = [KF(\text{iso-alkane } C_nH_{2n+2}) - KF(n-\text{alkane } C_nH_{2n+2})]/100 \qquad 2)$$

This factor is a negative number representing a normalized relative precedence of the peak of a hydrocarbon with respect to the peak of the normal alkane with the same carbon atom number.
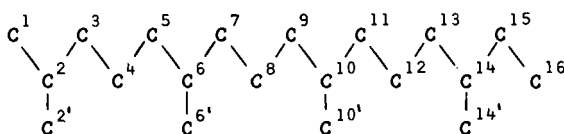
RESULTS AND DISCUSSION

Numbering of carbon atoms in the skeletons of the three isoprenoid molecules follows:
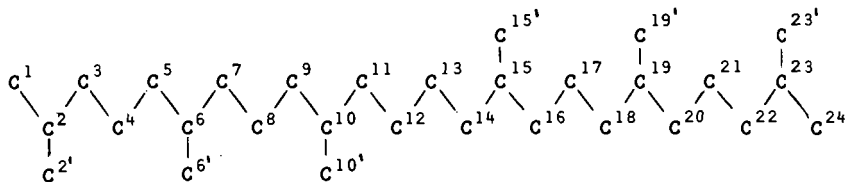
Pristane (2,6,10,14-tetramethylpentadecane)
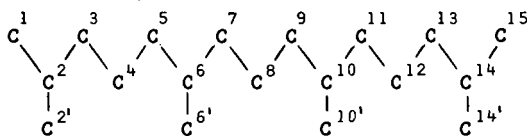
Phytane (2,6,10,14-tetramethylhexadecane)

Squalane (2,6,10,15,19,23-hexamethyltetracosane)

Conversions in the thermocracking reactions (250°C, 24 h) were: for pristane – 6.0%, for phytane – 2.7%, for squalane – 6.4%. Under these mild conditions only three stages of the radical chain reactions should be considered: formation of a parent radical, fission of the radical with the formation of an olefin and a smaller alkyl radical, and the chain transfer reaction yielding a low molecular weight alkane. One example of these three reactions involving a radical attack on the sixth position of the pristane molecule and the β-scission of the C_7-C_8 bond is:

421

Formation of a parent radical (hydrogen abstraction reaction):

$$R^\bullet \;+\; 2,6,10,14\text{-tetramethylpentadecane} \;\longrightarrow$$

3)

$$RH \;+\; CH_3\text{-}\underset{\underset{3}{CH_3}}{CH}\text{-}CH_2\text{-}CH_2\text{-}CH_2\text{-}\overset{\bullet}{\underset{\underset{3}{CH_3}}{C}}\text{-}CH_2\text{-}CH_2\text{-}CH_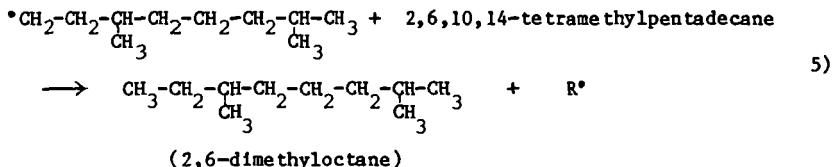2\text{-}\underset{\underset{3}{CH_3}}{CH}\text{-}CH_2\text{-}CH_2\text{-}CH_2\text{-}\underset{\underset{3}{CH_3}}{CH}\text{-}CH_3$$

β-scission reaction:

$$CH_3\text{-}\underset{\underset{3}{CH_3}}{CH}\text{-}CH_2\text{-}CH_2\text{-}CH_2\text{-}\overset{\bullet}{\underset{\underset{3}{CH_3}}{C}}\text{-}CH_2\text{-}CH_2\text{-}CH_2\text{-}\underset{\underset{3}{CH_3}}{CH}\text{-}CH_2\text{-}CH_2\text{-}CH_2\text{-}\underset{\underset{3}{CH_3}}{CH}\text{-}CH_3 \longrightarrow$$

4)

$$CH_3\text{-}\underset{\underset{3}{CH_3}}{CH}\text{-}CH_2\text{-}CH_2\text{-}CH_2\text{-}\underset{\underset{3}{CH_3}}{C}\text{=}CH_2 \;+\; {}^\bullet CH_2\text{-}CH_2\text{-}\underset{\underset{3}{CH_3}}{CH}\text{-}CH_2\text{-}CH_2\text{-}CH_2\text{-}\underset{\underset{3}{CH_3}}{CH}\text{-}CH_3$$
(2,6-dimethyl-1-heptene)

Chain transfer reaction:

$${}^\bullet CH_2\text{-}CH_2\text{-}\underset{\underset{3}{CH_3}}{CH}\text{-}CH_2\text{-}CH_2\text{-}CH_2\text{-}\underset{\underset{3}{CH_3}}{CH}\text{-}CH_3 \;+\; 2,6,10,14\text{-tetramethylpentadecane}$$

5)

$$\longrightarrow \quad CH_3\text{-}CH_2\text{-}\underset{\underset{3}{CH_3}}{CH}\text{-}CH_2\text{-}CH_2\text{-}CH_2\text{-}\underset{\underset{3}{CH_3}}{CH}\text{-}CH_3 \quad + \quad R^\bullet$$

(2,6-dimethyloctane)
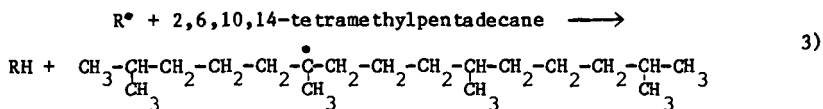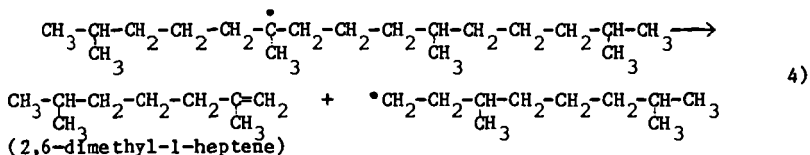
Reactions 3 and 5 are, in a general sense, the same reaction of hydrogen abstraction and they are separated here to emphasize chemistry of the reaction product formation. It is generally accepted (2, 4) that radical reactions of alkanes at low temperatures in the liquid state are accompanied by intramolecular radical isomerization (hydrogen atom shifts via five- and six-atom cyclic transition states) and by intermolecular hydrogen exchange reactions (reverse of reaction 3 with RH being the substrate molecule). The joint result of these two processes is the equilibrium distribution of primary radicals in terms of radical site positions, with the equilibrium being governed by relative radical stabilities.

Tables 1 and 2 list all possible alkanes and olefins which are formed in the principal thermocracking reactions of pristane, phytane, and squalane, experimental and calculated RRF values for the alkanes and olefins, and positions of radical attacks resulting in the formation of corresponding hydrocarbons. Peak areas for the products were used as the basis for the evaluation of reactivities of various bonds in two reactions - hydrogen abstraction (Reaction 3) and β-scission (Reaction 4).

β-scission reactions

In the majority of cases several β-scission reactions are possible for a radical formed in Reaction 3 (except for radicals in positions 2 in all isoprenoids and in position 16 for phytane). Analysis of reaction products allows estimation of probabilities of the scission reactions.

Tertiary radicals. Tertiary radicals in positions 6 and 10 are situated in very symmetrical environments. As a consequence,
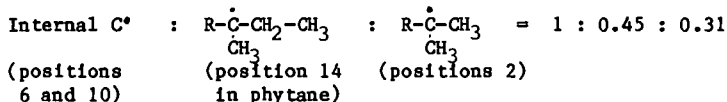
probabilities of β-scissions for the adjacent bonds are virtually equal. The ratios of products formed in the C_4-C_5 and C_7-C_8 bond scissions (radicals in position 6) are in the range 1.06-0.98 for all isoprenoids. The same ratios (1.08-0.99) were found for C_8-C_9 and C_{11}-C_{12} bond scissions in phytane and squalane (radicals in position 10). On the other hand, the probability of the CH_2-CH_2 bond (C_{12}-C_{13}) scission in the phytane radical (in position 14) is 10.6 times higher than that for the CH_2-CH_3 bond (C_{15}-C_{16}) which corresponds to the ΔE_{act} difference, ca. 2.5 kcal/mol.

Secondary radicals. Similarly to the previous case, if a secondary radical is situated in a symmetrical environment (positions 8 in all molecules, position 12 in phytane) the probability of the two β-scissions are identical (with precision ca. 4%) according to expectations. However even a slight deviation from the symmetry, in positions 4, results in a deviation from the equality. The ratio between the probabilities for the scisson of C_2-C_3 and C_5-C_6 bonds is ca. 0.63. When secondary radicals are in positions 7 (or positions 9 in phytane and squalane) the scission involves different chemical bonds. In these cases the ratios of the scission rates for the CH_2-CH_2 bonds (C_8-C_9 for radicals in positions 7) and for the CH_2-CH bonds (C_5-C_6) are ca. 0.71 (+7%). The same ratio (scission of C_{12}-C_{13} vs. C_9-C_{10}) for the phytane radical in position 11 is 0.58. However, the C_{12}-C_{13} bond in squalane is ca. 10% more reactive in β-scission than the C_9-C_{10} bond. Data for the pristane radical (in position 5) provide the most complete information of the relative probabilities of β-scission reactions. The ratios of the reactions for the CH_2-CH_2 bond (C_8-C_9), the CH_2-CH bond (C_5-C_6), and the CH_3-CH bond (C_6-$C_{6'}$) are 4.72 : 6.70 : 1.

Reactivities of C-H bonds in hydrogen abstraction reactions

Tertiary C-H bonds

Tertiary C-H bonds are the most active in radical hydrogen abstraction reactions as emphasized by their low bond energies, ca. 90 kcal/mol (2, 4). Our data show that reactivities of the C-H bonds in 6 and 10 positions are equal for all three isoprenoids (corresponding product yields are in the range 1.00-1.03). The ratios of products formed from the end- and internal tertiary radicals are:

$$\text{Internal } C^\bullet \quad : \quad R\text{-}\overset{\bullet}{C}\text{-}CH_2\text{-}CH_3 \quad : \quad R\text{-}\overset{\bullet}{C}\text{-}CH_3 \quad = \quad 1 : 0.45 : 0.31$$
$$\underset{CH_3}{} \qquad \underset{CH_3}{}$$

(positions   (position 14   (positions 2)
 6 and 10)   in phytane)

If one takes into account different scission patterns for these radicals (discussed earlier) and the exsitence of only one β-scission route for the end-tertiary radicals these ratios translate into the ratios of formation rates for corresponding radicals ca. 1 : 0.7 : 0.8.

Secondary radicals

The isoprenoids studied can form several structurally different secondary radicals.
Radicals -CH_2-$\overset{\bullet}{C}H$-CH_2-. As expected, the radicals in positions 4 and 12 in the phytane molecule have the same reactivity (the corresponding

product ratio is 1.05). However, these radicals positioned in the center
of the molecules (positions 8) are slightly more reactive than similar
radicals in positions 4: the reactivity ratios are 1.3 for pristane, 1.2
for phytane, and 1.7 for squalane. Reactivity of the secondary radical
in position 12 of squalane is 2.4 times less than that of a similarly
situated radical in position 8.

Radicals $-CH_2-CH-CH-$. Reactivities of all radicals in positions 5, 7, 9,
and 11 in the molecules are equal within ±10%.

Relative reactivities of various secondary radicals. Significant diffe-
rences between reactivities of differently flanked secondary radicals
were found for all isoprenoids. Radicals $-CH_2-CH-CH_2-$ are 4.8 times (±10%)
more reactive than $CH_2-CH-CH-$ radicals. The only exception was found
for squalane: reactivity of the radical in position 12 is only 2.3 times
higher than reactivity of the radical in position 11.

Primary radicals

Information on relative reactivity of primary radicals is limited
due to difficulties in identification of the products of their β-scission
and due to low content of the products. In the case of phytane the
radical in position 6' has the same reactivity as the radical in position
14' and it is ca. 20% less reactive than the radical in position 10'.

The yields of scission products from the primary radicals in positions
1 are ca. 2 times less than those for the radicals in positions 6'. If one
takes into account that only one scission route is available for the first
radicals, it can be concluded that reactivities of all primary radicals
in the isoprenoids are very close.

Comparisons of reactivities of various radicals

Comparisons of the yields of products from β-scissions of radicals
of various structures allows approximate evaluation of their relative
reactivities.

Primary radicals $\overset{\bullet}{C}H_2-CH-$ vs. secondary radicals $-CH_2-\overset{\bullet}{C}H-CH_2-$. The pro-
duct ratio for scission of corresponding radicals for all isoprenoids is
ca. 0.067. If one takes into account the differences between the numbers
of C-H bonds in these groups, the ratios of reactivities of C-H bonds in
the methyl group (CH_3-CH-) and the central methylene group in the sequence
$CH(CH_3)-CH_2-CH_2-CH_2-CH(CH_3)$ is ca. 0.045 which corresponds to ΔE_{act} ca.
-3.2 kcal/mol.

Primary radicals $\overset{\bullet}{C}H_2-CH-$ vs. secondary radicals $-CH_2-\overset{\bullet}{C}H-CH-$. The pro-
duct ratio for scission of corresponding radicals for all isoprenoids is
ca. 0.27 which translates into the difference between reactivities of
corresponding C-H bonds ca. 0.18 and ΔE_{act} ca. -1.8 kcal/mol.

Secondary radicals vs. tertiary radicals $CH_2-\overset{\bullet}{C}(CH_3)-CH_2-$. The product
ratio for scission of secondary radicals (in positions 8) and that for
the tertiary radicals in positions 6 or 10 is 0.89. This corresponds
to the ratio of ca. 2.25 for C-H bond reactivities in hydrogen abstraction
reactions involving the tertiary CH_3-CH- groups and the central methylene
groups in the isoprenoids (positions 8). Corresponding ΔE_{act} is ca.
0.8 kcal/mol. As was mentioned before, central CH_2 groups in $-CH_2-CH_2-CH-$
sequences are less reactive than in $-CH_2-CH_2-CH_2-$ sequences. For them
the corresponding C-H bond reactivity ratio is 11.6 and ΔE_{act} is ca.
2.6 kcal/mol.

1. A. Kossiakoff, F. O. Rice, J. Am. Chem. Soc., 65, 590 (1943).
2. Free Radicals (vols. I and II), J. K. Kochi, Ed., J. Wiley, New York, 1973.
3. S. W. Benson, The Foundations of Chemical Kinetics, McGraw-Hill, New York, 1960, p.343.
4. E. Ranzi, M. Dente, S. Pierucci, G. Biardi, Ind. Eng. Chem., Fundam., 22, 132 (1983).
5. Y. V. Kissin, G. P. Feulmer, J. Chromat. Sci., in press.
6. Y. V. Kissin, J. Chromat. Sci., in press.
7. G.I. Spivakovskii, A.I. Tishchenko, I.I. Zaslavskii, N.S. Wulfson, J. Chromatoraphy, 144, 1 (1977).
8. E. Kovats, Z. Anal. Chem., 181, 351 (1961).

Table 1

ALKANES FORMED IN THERMOCRACKING REACTIONS OF PRISTANE, PHYTANE, AND SQUALANE AT 250°C †

Alkane	Formed from			RRF (exp.)	RRF (calc.)	ΔRRF %
	Pristane	Phytane	Squalane			
	(position of radical attack)					
$n-C_4$		*(12)				
$iso-C_4$	*(5)	*(5)	*(5)			
$2-Me-C_4$	*(6)	*(6,11)	*(6)			
$2-Me-C_5$	*(6',7)	*(6',7)	*(6',7)			
$3-Me-C_5$		*(10)				
$3-Me-C_6$		*(9,10')				
$2-Me-C_7$	*(8)	*(8)	*(8)			
$2,6-Me_2-C_7$	*(9)	*(9)	*(9)	-0.700	-0.700	0.0%
$3-Me-C_8$		*(8)				
$2,6-Me_2-C_8$	*(6)	*(7,10)	*(10)	-0.636	-0.644	1.2%
$2,6-Me_2-C_9$	*(5,10')	*(10',11)	*(10',11)	-0.747	-0.736	-1.5%
$3,7-Me_2-C_9$		*(6)		-0.578	-0.568	-1.7%
$3,7-Me_2-C_{10}$		*(5,6')		-0.695	-0.674	-3.0%
$2,6-Me_2-C_{11}$	*(4)	*(12)	*(12)	-0.833	-0.812	-2.5%
$2,6,10-Me_3-C_{11}$	*(3)	*(13)	*(12)	-1.252	-1.175	-6.1%
$3,7-Me_2-C_{12}$		*(4)		-0.788	-0.753	-4.5%
$2,6,10-Me_3-C_{12}$	*(2,14)	*(3,14)	*(11)	-1.199	-1.114	-7.1%
$2,6,10-Me_3-C_{13}$	*(1,2')	*(14',15)	*(10)	-1.353	-1.254	-7.3%
$3,7,11-Me_3-C_{13}$		*(2)		-1.150	-1.076	-6.4%
$2,6,10-Me_3-C_{14}$			*(9,10')	-1.430	-1.329	-7.1%
$3,7,11-Me_3-C_{14}$		*(1)		-1.300	-1.210	-7.0%
$2,6,10-Me_3-C_{15}$		*(16)		-1.477	-1.386	-6.2%
$2,6,10-Me_3-C_{16}$			*(8)	-1.531	-1.407	-8.1%
$2,6,10,15-Me_4-C_{16}$			*(7)	-1.940	-1.788	-7.9%
$2,6,10,15-Me_4-C_{17}$			*(6)	-1.862	-1.705	-8.5%
$2,6,10,15-Me_4-C_{18}$			*(5,6')	-2.102	-1.880	-10.6%
$2,6,10,15-Me_4-C_{20}$			*(4)	-2.115	-2.063	-2.5%
$2,6,10,15,19-Me_5-C_{20}$			*(3)	-2.345	-2.464	5.1%
$2,6,10,15,19-Me_5-C_{21}$			*(2)	-2.320	-2.408	3.8%
$2,6,10,15,19-Me_5-C_{22}$			*(1)	-2.455	-2.608	6.2%

† amounts of methane, ethana, and propane cannot be determined quantitatively and are not reported in the table.

Table 2

OLEFINS FORMED IN THERMOCRACKING REACTIONS OF PRISTANE, PHYTANE, AND SQUALANE AT 250°C †

Olefin	Formed from			RRF (exp.)	RRF (calc.)	ΔRRF %
	Pristane	Phytane	Squalane			
	(position of radical attack)					
$C_3^=$	*(1)	*(1)	*(1)			
$1-C_4^=$		*(14')				
$2-C_4^=$		*(14')				
$iso-C_4^=$	*(2)	*(2)	*(2)			
$2-Me-1-C_4^=$		*(14)				
$3-Me-1-C_4^=$	*(3)	*(3)	*(3)			
$3-Me-1-C_5^=$		*(13)				
$4-Me-1-C_5^=$	*(4)	*(4)	*(4)			
$4-Me-1-C_6^=$		*(12)				
$6-Me-1-C_7^=$	*(6')	*(6')	*(6')			
$6-Me-2-C_7^=$	*(5)	*(5)	*(5)			
$6-Me-1-C_8^=$		*(10')				
$6-Me-2-C_8^=$		*(11)		-0.228		
$2,6-Me_2-1-C_7^=$	*(6)	*(6)	*(6)	-0.520	-0.518	0.4%
$2,6-Me_2-1-C_8^=$		*(10)		-0.455	-0.455	0.0%
$3,7-Me_2-1-C_8^=$	*(7)	*(7)	*(7)	-0.896	-0.880	1.8%
$3,7-Me_2-1-C_9^=$		*(9)			-0.803	
$4,8-Me_2-1-C_9^=$	*(8)	*(8)	*(8)	-0.850	-0.846	0.5%
$4,8-Me_2-1-C_{10}^=$		*(8)		-0.796	-0.785	1.4%
$6,10-Me_2-1-C_{11}^=$	*(6')	*(6',10')	*(10')	-0.915	-0.916	0.1%
$6,10-Me_2-2-C_{11}^=$	*(7)	*(9)	*(9)	-0.799	-0.812	1.6%
$6,10-Me_2-2-C_{12}^=$		*(7)		-0.751	-0.740	4.1%
$2,6,10-Me_3-1-C_{11}^=$	*(6)	*(10)	*(10)	-1.047	-1.008	3.7%
$3,7,11-Me_3-1-C_{12}^=$	*(5)	*(11)	*(11)	-1.459	-1.328	9.0%
$2,6,10-Me_3-1-C_{12}^=$		*(6)		-0.992	-0.920	7.2%
$4,8,12-Me_3-1-C_{13}^=$	*(4)	*(12)	*(12)	-1.436	-1.338	6.8%
$3,7,11-Me_3-1-C_{13}^=$		*(5)		-1.398	-1.287	7.9%
$4,8,12-Me_3-1-C_{14}^=$		*(4)		-1.379	-1.301	5.6%
$5,9,13-Me_3-1-C_{14}^=$			*(12)	-1.505	-1.420	5.6%
$6,10,14-Me_3-1-C_{15}^=$	*(1)	*(14')			-1.474	
$6,10,14-Me_3-2-C_{15}^=$	*(3)	*(13)				
$2,10,14-Me_3-5-C_{15}^=$	*(5)					
$2,10,14-Me_3-6-C_{15}^=$	*(7)					
$6,10,14-Me_3-1-C_{16}^=$		*(1)			-1.409	
$6,10,14-Me_3-2-C_{16}^=$		*(3)			-1.326	
$2,10,14-Me_3-5-C_{16}^=$		*(5)			-1.241	
$2,10,14-Me_3-6-C_{16}^=$		*(7)			-1.241	
$3,11,15-Me_3-6-C_{16}^=$		*(11)			-1.227	
$3,11,15-Me_3-7-C_{16}^=$		*(9)			-1.227	
$7,11,15-Me_3-1-C_{16}^=$			*(10')	-1.583	-1.494	5.6%
$7,11,15-Me_3-2-C_{16}^=$		*(15)	*(11)	-1.530	-1.411	7.7%
$7,11,15-Me_3-3-C_{16}^=$		*(13)				
$2,6,10,14-Me_4-1-C_{15}^=$			*(14)		-1.525	
$2,7,11,15-Me_4-1-C_{16}^=$			*(10)	-1.712	-1.562	8.8%
$3,8,12,16-Me_4-1-C_{17}^=$			*(9)	-2.114	-1.909	9.7%
$4,9,13,17-Me_4-1-C_{18}^=$			*(8)	-2.00	-1.963	2.0%
$6,11,15,19-Me_4-1-C_{20}^=$			*(6')		-2.19	
$6,11,15,19-Me_4-2-C_{20}^=$			*(7)		-2.13	
$2,6,11,15,19-Me_5-2-C_{20}^=$			*(6)	-2.14	-2.18	1.9%

† olefins $C_{26}-C_{29}$ in the products of squalane thermocracking were not identified quantitatively and are not reported in the table.

USE OF THE STRUCTURE-CHEMICAL REACTIVITY DATA FOR
DEVELOPMENT OF NEW METHODS IN PETROLEUM HEAVY ENDS UPGRADING

M. Farcasiu, E. J. Y. Scott and R. B. LaPierre

Mobil Research and Development Corporation
Central Research Laboratory
P. O. Box 1025, Princeton, New Jersey 08540

INTRODUCTION

The chemical structure of the heavy ends of petroleum has been
studied extensively (1). However, these studies have had little
impact on the processes used commercially to upgrade heavy
petroleum fractions. Industrial processes involve thermal (high
temperature free radical chemistry) or catalytic routes such as
catalytic cracking or hydroprocessing at temperatures greater
than 300°C.

Low temperature ionic reactions have not been explored
extensively for upgrading petroleum heavy ends. We have examined
transalkylation, the transfer of alkyl fragments from high
molecular weight components to smaller aromatic acceptor
molecules in presence of Friedel Craft catalysts. We present
results of transalkylation using catalysts consisting of
trifluoromethanesulfonic acid as well as aluminum chloride
promoted by water (2). Results are presented for transalkylation
to native aromatic compounds present in crude petroleum (whole
crude transalkylation) as well as to added aromatic molecules
(resid transalkylation).

Most molecules in petroleum heavy ends contain 20 to 40 wt.%
aliphatic groups substituted to aromatic (or heteroaromatic)
rings (3). These aliphatic substituents are:

- normal and iso alkyl groups (we positively identified C_2
  to C_{16} alkyl chains);
- cycloalkyl groups (we identified cyclopentyl and
  cyclohexyl substituents but the presence of larger
  saturated polycyclic groups cannot be precluded);
- methylene groups linking two aromatic rings.

In the presence of Friedel Crafts catalysts these aliphatic
groups can be transferred to small aromatic molecules (3). The
result of transalkylation is then the formation of new
distillable products which contain the small aromatic molecules
substituted with normal, iso, and cyclo alkyl groups. Obviously,
in such complicated mixtures as the petroleum heavy ends are,
under the transalkylation reaction conditions, other reactions
will also take place; for example, the dialkyl sulfides form
mercaptanes and paraffins, and at long reaction times, alkyl
substituents with five or more carbons form hydroaromatic rings
by cyclization.

The products of the transalkylation and of secondary reactions
are mixtures of petroleum like compounds with molecular weights

427

(and boiling points) ranging from that of the acceptor (the small aromatic molecule) to that of the resid.

If whole crude oils are treated under the conditions of the transalkylation reaction, alkyl groups from heavy ends are transferred to the light aromatic hydrocarbons present in the crude oil. The result is a change of the boiling point distribution of the whole crude toward medium boiling point fractions.

Very early in our work we realized the lack of literature data concerning the transfer of the alkyl substituents between aromatic rings with different degrees of ring condensation. To gain this information we studied the transalkylation reaction with appropriate model compounds (3,4).

The transalkylation reaction can be applied both to materials soluble in aromatics and to solids as kerogens (3) or coals (5,6) and coal liquefaction products (6).

RESULTS AND DISCUSSION

The transalkylation reaction can be formulated:

$$Ar^I\text{-}Alkyl^I + Ar^{II}H \rightleftharpoons Ar^IH + Ar^{II}\text{-}Alkyl^I$$

In our discussion $Ar^I\text{-}Alkyl^I$ will denote large aromatic molecules from petroleum heavy ends and $Ar^{II}H$ will be benzene, toluene or o-xylene.

A. Kinetic and thermodynamic constraints of the transalkylation reaction

We have shown previously (3,4) that the rate of the transalkylation reaction between polyaromatic and monoaromatic rings is:

-   independent of the chain length (at least for C_2-C_{10} alkyl chains),
-   dependent on the nature of the aliphatic substituent (cycloalkyls transfer faster than n-alkyls),
-   dependent on the structure of the polyaromatic moiety involved in the transalkylation reaction (the rate of transfer of the aliphatic substituent increases for systems with increased degree of aromatic ring condensation).

Concerning the thermodynamics of transalkylation, we found that the thermodynamic equilibrium is:

-   independent of the structure of the polyaromatic moiety (Table I),
-   only slightly influenced by temperature in the 27-227°C interval in which we studied the transalkylation reaction (Table II).

Data in Tables I and II show that the equilibrium constant of the

transalkylation reaction is close to unity (i.e. ΔG = 0) for any pair of donor-acceptor. That means that at donor-acceptor molar ratio of 1:1, the maximum conversion to be expected is 50% for any of the starting materials. Thus, the only way to push a transalkylation reaction in a desired direction is to work with excess of acceptor. For example, for a molar ratio of 1:4 at equilibrium, 80% of donor will be converted at 127°C (400°K).

In the case of conversion of petroleum heavy ends by a transalkylation reaction, the big differences between the molecular weight of the donor (average molecular weight 1000) and of the acceptor (molecular weight ~100) insure an advantageous molar ratio even for a weight ratio resid:aromatic hydrocarbon of 1:1.

These thermodynamic constraints are very important for upgrading whole crude (see Section C following).

While the thermodynamic equilibrium is independent of the degree of aromatic ring condensation of the donor, the rates of the transalkylation reaction are faster for transfer of aliphatic groups from more to less condensed aromatic systems. The transfer in the opposite direction necessitates larger acid (catalyst) concentration (4), which in turn favors some secondary reactions.

B. Transalkylation reactions of vacuum resids

Some transalkylation reactions between Arabian Light vacuum resid and toluene or o-xylene are given in Table III. Typical composition of the distillate is shown in Figure 1 for an Alaskan resid. Some properties of the dealkylated resids are given in Table IV. In general, 60-80% of the initial resid remains as dealkylated resid.

If the dealkylated resid is hydrotreated in the presence of Co-Mo catalysts (Table V), the hydrogen consumption is similar to that for the untreated resid, but the degree of desulfurization is somewhat higher (72%) for the dealkylated resid than for the untreated resid (65% desulfurization). It should be observed that the dealkylated resid (76% of the initial resid) was distilled to a lower average molecular weight (620) than that of untreated resid (average molecular weight 1100).

The saturated hydrocarbon fraction in the hydrotreated vacuum resid (for the hydrotreating condition see Table V) represents 20.5% of the product and has an average molecular weight of ~1000. In the hydrotreated dealkylated resid the saturated hydrocarbons represent 24.5% of the product and their average molecular weight is only 386.

C. Transalkylation reactions of whole crude oils

The transfer of aliphatic substituents from the big molecules to lower molecular weight aromatics of a crude oil can be achieved under mild conditions in the presence of a Friedel-Crafts catalyst (Table VI). We used topped (80°C+) crude oils because the lowest boiling point acceptor in crude oils is benzene

(b.p.~80°C). Work with model compounds (4) indicated that the transfer of substituents is easier from polyaromatic to monoaromatic rings. This favors the redistribution of aliphatic substituents in whole crudes in the desired direction.

In the case of aromatic crudes (for example the Alaskan crude in Table VI), there are enough low molecular weight natural acceptors in the crude to achieve a substantial transfer. In the case of a paraffinic crude (North Sea crude), the addition of some small aromatic molecules can be helpful (Table VI).

The net result of the internal transalkylation is a redistribution of boiling points in the crude with an increase in the quantity of medium range products.

D. Chemical composition and mechanistic limitations of upgrading petroleum heavy ends by the transalkylation reaction

The petroleum heavy ends contain large amounts of aliphatic substituents on polyaromatic rings. This makes the use of the transalkylation reaction an attractive alternative for their upgrading.

One element of structure which poses a problem is the presence of basic compounds, especially basic nitrogen compounds in petroleum heavy ends. The basic nitrogen compounds react with the acidic catalysts and form salts.

Another limitation for the use of the transalkylation reaction is the effect of acid concentration on the reaction rate. Our work with model compounds (4) has shown that the concentration of acid must exceed a certain threshold to obtain an acceptable rate of reaction.

Understanding of the quantitative relationship between the chemical structure of the reactants and the concentration of acid is new chemistry and our initial results (4) are only a beginning. Certainly, more research in this area is needed because it is likely to be relevant to other acid catalyzed reactions besides transalkylation.
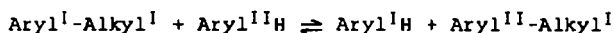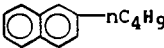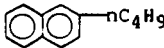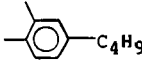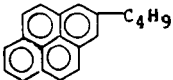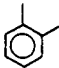
REFERENCES
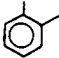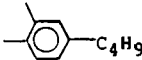
1. Speight, J. G., "The Chemistry and Technology of Petroleum", M. Dekker, Inc., New York, 1980, and references therein.

2. Farcasiu, M., U.S. Patent 4,317,712, March 2, 1982.

3. Farcasiu, M, Forbus, T. R., LaPierre, R. B., ACS Petr. Chem. Div. Preprints 28, 279 (1983).

4. Farcasiu, M.,Forbus, T. R., Rubin, B. R., paper submitted to J. Org.Chem.

5. Benjamin, B. M., Douglas, E. C., Canonico, D. M., Fuel <u>63</u>, 1130 (1984).

6. Farcasiu, M., Proceedings of the Symposium on Chemistry of Coal Liquefaction and Catalysis, March 17-20, 1985, Sapporo, Japan.

7. Stull, D. R., Westrum, Jr., E. F. and Sinke, G. C., "The Chemical Thermodynamics of Organic Compounds", John Wiley (1969).

8. Benson, S. W., "Thermochemical Kinetics", Chapter 2, John Wiley (1968).

9. Stein, S. E., Golden, D. M. and Benson, S. W., J. Phys. Chem <u>81</u>, 314 (1977).

TABLE I

Equilibrium Constants at 400°K (127°C) for Several Transalkylation Reactions

$$Aryl^I\text{-}Alkyl^I + Aryl^{II}H \rightleftharpoons Aryl^I H + Aryl^{II}\text{-}Alkyl^I$$

$Aryl^I$-$Alkyl^I$ donor	$Aryl^{II}H$ acceptor	$\Delta G°$ 400°K Kcal/mole	$K_{400°K}$
$-nC_4H_9$		-0.11	1.15
$-nC_4H_9$		-0.11	1.15
$-C_4H_9$		0	~1
$-C_4H_9$		+0.11	0.87
$-C_4H_9$		0	~1

$\Delta G°$ values for 2 n-butyl naphthalene, benzene and o-xylene are experimental values (7), those for 1,2-dimethyl 4-n-butyl benzene and 2-n-butyl pyrene are calculated by the method of "group additivity" (8,9).

TABLE II

The Influence of Temperature on Thermodynamical

Equilibrium of the Transalkylation Reaction*

Equilibrium Constant at:

300°K (27°C)	400°K (127°C)	500°K (227°C)
1.03	1.15	1.21

*All values are experimental values (7).

TABLE III

Conditions of the Transalkylation Reaction

Vacuum Resid (1050+F) a	Aromatic Hydro- carbon b	Catalyst c	Wt. Ratio a:b:c	Temp. °C	Time Hrs.	Wt.% Distil- late[a](based on resid)
1. Arabian Light	toluene	$AlCl_3$	1:6.5:0.5	20	18	10
2. Arabian Light	o-xylene	$AlCl_3$	1:0.86:0.5	144	3	15.3
3. Dealky- lated Resid Exp.2	o-xylene	$AlCl_3$	1:1.7:0.5	144	6	25
4. Arabian Light	o-xylene	CF_3SO_3H	1:2.6:0.4	144	6	34

[a]This % includes the light aromatics incorporated by transalkylation.

TABLE IV

Properties of Dealkylated Resids

	Wt.%			MW	
	C	H	S	VPO/Toluene	% ar H
Arabian Light	85.1	10.4	4.0	1100	5.6
Dealkylated Resid exp. 2 Table IvII	86.5	9.6	4.1	620	~11[a]
Dealkylated Resid exp. 3 Table III	87.3	8.7	3.7	503	--

[a]The value of % ar H (^{1}HNMR) is from a similar transalkylation run.

TABLE V

Chemical and Structural Properties of Hydrotreated Arabian Light Vacuum Resid and Hydrotreated Dealkylated Arabian Light Resid

Hydrotreating Conditions: wt.ratio resid:o-xylene:CoMo (HDS1441) catalyst 1:344:0.5; t = 340°C; 1000 psi H_2, 1 h

Material	%arH	Elem. Analysis Wt.%			Av. M_W
		C	H	S	(VPO Toluene)
1. Arabian Light Vac. Resid	5.6	85.1	10.4	4.0	1110
2. Hydrotreated 1 (yield 90% of 1)	1.6	86.5	11.7	1.4	1000
3. Dealkylated (AlCl$_3$ catalyst) Arabian Light Vacuum Resid (76% of initial material)	9.8	84.9	9.1	3.6	620
4. Hydrotreated 3 (yield 90% of 3)	6.8	88.2	10.5	1.0	477

TABLE VI

Boiling Point Distribution of Topped Whole Crude Oils
Before and After Transalkylation in the Presence of
Trifluromethanesolfonic Acid*

	Boiling Points, °C			
	80-215	215-344	349-426	426+
Topped Alaskan Crude				
Initial	7.9	26.9	17.0	48.2
After transalkylation	9.3	32.0	19.7	39.0
	+1.4	+5.1	+2.7	-9.2
Topped North Sea Crude				
Initial	10.5	35.1	22.0	32.4
After transalkylation	11.7	37.1	24.1	27.1
Δ	+1.2	+2.0	+2.1	-5.3
Topped North Sea Crude 5% o-Xylene				
Initial	15.5	33.4	21.0	30.8
After transalkylation	12.6	40.2	26.3	20.9
Δ	-2.9	+6.8	+5.3	-9.9

*Typical transalkylation conditions: wt. ratio oil : CF_3SO_3H
10:1, reaction temperature ⁻100°C, reaction time ⁻4 h. After
reaction, the mixture was quenched with aqueous NaOH, the organic
layer was separated and dried over $MgSO_4$. The boiling point
distribution in the initial material and products was determined
by flash distillation over chromosorb followed by simulated
distillation by gas chromatography.

FIGURE 1.

GAS CHROMATOGRAM OF THE TRANSALKYLATED PRODUCTS FROM
THE REACTION BETWEEN AN ALASKAN VACUUM RESID AND o-XYLENE